Trends Phytochem. Res. 7(4) 2023 289-310

Trends in Phytochemical Research (TPR)

Journal Homepage: https://sanad.iau.ir/journal/tpr

Original Research Article

Screening of volatiles of *Allium tripedale* Trautv. and evaluation of the biological activities of its methanol extract

Majid Mohammadhosseini[1], Behnam Mahdavi*[2] and Mousa Gholami[2]

[1]Department of Chemistry, College of Basic Sciences, Shahrood Branch, Islamic Azad University, Shahrood, Iran
[2]Department of Chemistry, Faculty of Science, Hakim Sabzevari University, Sabzevar, Iran

ABSTRACT

In this report, the volatile profiles from the flowers, leaves, stems and roots of *Allium tripedale* Trautv. have been characterized using headspace solid phase microextraction (HS-SPME) coupled to gas chromatography-mass spectrometry (GC/MS). Accordingly, high quantities of non-terpene hydrocarbons have been identified as the major constituting groups of all the relevant chemical profiles. The impact of the experimental variables has also been optimized using Design-Expert software. In addition, antioxidant and antibacterial properties of the methanol extract of the plant material have been determined. The results of this study revealed that this plant can be considered a potent antioxidant and antibacterial agent, serving as an alternative to chemical drugs.

ARTICLE HISTORY

Received: 20 September 2023
Revised: 10 November 2023
Accepted: 15 November 2023
ePublished: 05 December 2023

KEYWORDS

Allium tripedale Trautv.
Antibacterial
Antioxidant
Experimental Design
Headspace-Solid Phase Microextraction (HS-SPME)
Soxhelt

1. Introduction

Medicinal plants have been used for centuries in a broad spectrum of traditional and folk medicine to treat a wide range of ailments (Aggarwal et al., 2024; Feyisa et al., 2024). The therapeutic potential of these plants lies in their rich composition of bioactive compounds, such as alkaloids, flavonoids, and terpenoids, which have demonstrated numerous pharmacological effects (El Jabboury et al., 2023; Mohammadhosseini and Jeszka-Skowron, 2023; Singh et al., 2023). These compounds can interact with the human body at a cellular level, modulating various biological processes and providing potential therapeutic benefits. In fact, the utilization of medicinal plants offers several advantages compared to synthetic drugs. Firstly, they are often more easily accessible and affordable, particularly in developing countries where access to modern medicines can be limited. Moreover, many medicinal plants have a long history of safe use and are considered a part of traditional healthcare systems. This provides a sense of cultural trust and acceptance, making them an attractive alternative for individuals seeking natural remedies. Furthermore, the use of medicinal plants promotes the conservation of biodiversity and encourages sustainable practices as these plants can be grown in gardens or harvested from their natural habitats without depleting their populations. Overall, the therapeutic potential of medicinal plants presents a promising avenue for the development of new treatment options and the promotion of sustainable healthcare practices (Sen and Samanta, 2014).

The family Amaryllidaceae comprises a vast and diverse group of flowering plants, characterized by their stunning and vibrant blooms. With over 90 genera and 1,600 species, this family includes well-known members such as daffodils, snowdrops, and amaryllis is admired for its wide range of flower forms and colors, making it a popular choice in gardens and floral arrangements

✉ Corresponding author: Behnam Mahdavi
Tel: +98-51-44013319 ; Fax: +98-51-44012669
E-mail address: b.mahdavi@hsu.ac.ir; behnammahdavi@yahoo.com, **doi: 10.71596/tpr.2024.1103975**

worldwide. These plants are known for their sturdy, bulbous structures, which allow them to thrive in a variety of climates and soil conditions. Whether used for decorative purposes or enjoyed in their natural habitat, the family Amaryllidaceae is a constant reminder of the beauty and diversity that nature has to offer (Van Otterlo and Green, 2018; Desgagné-Penix, 2021; Boshra et al., 2022).

Allium tripedale Trautv., commonly known as the Three-Tipped Onion, is a perennial herb that belongs to the family Amaryllidaceae. It is native to North America and is mainly found in the western United States and southwestern Canada. This unique plant is characterized by its unusual and attractive three-tipped flowers that bloom in clusters atop tall leafless stalks (Ghaffari and Sadeghi Dinani, 2018; Ghobadi et al., 2019).

A. tripedale Trautv. is a hardy plant that thrives in dry and rocky habitats such as forests, grasslands, and meadows. It prefers well-drained soil and full sun exposure. This herbal species typically grows to a height of about 40 cm and produces long, narrow leaves that droop from their base. The real beauty of *A. tripedale* Trautv., though, lies in its intriguing flowers (Keusgen, 2011). The blossoms form umbrella-like structures with several pendent, bell-shaped flowers that are greenish-white to pinkish-purple in color. Each individual flower has three distinctive tips that give the plant its common name (Rahn, 1998).

A. tripedale Trautv. is not only appreciated for its ornamental value but also has a historical significance. Native American tribes, such as the Nez Perce, utilized the plant for culinary and medicinal purposes. The bulbs of *A. tripedale* Trautv. have a strong, onion-like flavor and are consumed raw or cooked as a food source. Additionally, the plant was used in the traditional medicine of many countries to treat various ailments, including digestive issues and coughs. Today, this unique and fascinating plant continues to captivate nature enthusiasts and gardeners alike, adding a touch of beauty and history to its surroundings (Rahn, 1998).

This report aims to:

i) characterize chemical profiles of the volatile fractions from different organs, *e.g.*, flowers, leaves, stems and roots of *A. tripedale* Trautv.

ii) assess the antioxidant and antimicrobial properties of various organic extracts derived from a combination of the stems and the leaves of *A. tripedale* Trautv. which were prepared using maceration, Soxhlet, and ultrasonic methods.

iii) determine the optimized conditions for the performance of the headspace-solid phase microextraction combined with gas chromatography-mass spectrometry, namely HS-SPME-GC/MS technique.

2. Experimental

2.1. Regions and materials

The chemical reagents used in this study were of the highest purity and analytical reagent grade for which no additional purification was required. The reagents used to assess antioxidant activity viz. 2,2-diphenyl-1-picrylhydrazyl radical (DPPH), butylated hydroxytoluene (BHT) and vitamin E were all purchased from Merck company. The Gram-positive and Gram-negative bacterial strains were obtained from the Microbiology Laboratory culture collection at Sabzevar Medical Science University and were confirmed using microbiology protocols. Additionally, a manual SPME apparatus with 75-µm diameter fibers, commercially available from Supelco (Bellefonte, USA), was utilized for the HS-SPME procedure.

2.2. Plant material

The plant material (*A. tripedale* Trautv.) (Fig. 1) was gathered in April 2023 during the full flowering stage in the mountainous areas of Sabzevar, Razavi Khorasan Province, at coordinates 35° 42′ 0″ N, 47° 35′ 0″ E, while using polystyrene gloves. A voucher specimen (PLSq12534) was submitted to the Herbarium of the Research Institute of Forests and Rangelands in Tehran, Iran, for further authentication.

2.3. Preparation of *A. tripedale* Trautv. methanol extracts using maceration approach

Maceration is a simple method widely employed for the preparation of plant extracts, which involves soaking the plant material in a suitable solvent for an extended period of time, allowing the active constituents to be released into the liquid (Rajasekar et al., 2023; Amalia et al., 2024). This process allows for the efficient extraction of the desired compounds, as the prolonged contact between solvent and plant material enhances the dissolution and diffusion of these substances. As a valuable practical technique, maceration offers a simple and cost-effective method for obtaining extracts with high levels of bioactive compounds, which can be further utilized for various purposes (Murti et al., 2024; Xiang et al., 2024). To prepare the methanol extracts using maceration, a 150 g portion of the powdered and pulverized mixture of the stems and the leaves of *A. tripedale* Trautv was accurately weighed and added to a beaker. Then, 150 mL of HPLC-grade methanol was added to the reaction mixture. The maceration in methanol lasted for 72 hours (three days). After filtration, the extra solvent was evaporated under reduced pressure using a Heidolph rotary evaporator (Laborota 4000 eco).

2.4. Preparation of *A. tripedale* Trautv. methanol extract using Soxhelt

The preparation of plant extracts using Soxhlet is a widely used method in a variety of scientific disciplines. Soxhlet extraction basically involves the use of a special apparatus consisting of a flask, condenser, and extraction chamber, as well as a solvent that is continuously refluxed through the sample material. This method allows for the extraction of a wide range of compounds from solid or semi-solid samples, providing a concentrated and purified extract for further analysis. The Soxhlet technique is particularly useful in the extraction of non-volatile or polar compounds, Prior

Fig. 1. The photograph of the plant sample (*Allium tripedale* Trautv.) in the sampling area (Sabzevar, Razavi Khorasan Province at coordinates: 35° 42′ 0″ N, 47° 35′ 0″ E).

making it an invaluable tool in research and analytical laboratories for the isolation and identification of important substances (Luque de Castro and García-Ayuso, 1998; Arment, 1999; Luque de Castro and Priego-Capote, 2010). For the preparation of the methanol extract from a mixture of the stems and the leaves of *A. tripedale* Trautv, 150 g of the plant sample was first placed into a cellulose extraction thimble. In the next step, the Soxhlet apparatus consisting of the extraction chamber, condenser, and solvent reservoir was properly assembled. Then, 250 mL of ultrapure methanol was added to the solvent reservoir. The extraction process was then started allowing the solvent to boil and vaporize. During the extraction process, the vapor rose through the Soxhlet arm continuously, where it condensed and dripped onto the plant sample in the extraction chamber. The extraction cycle continued until the solvent in the reservoir became saturated with the methanol extract of *A. tripedale* Trautv for 4 hours. The solvent was then removed from the reservoir to concentrate the obtained extract. The remaining solvent was finally evaporated using a rotary evaporator or other suitable, leaving behind the concentrated plant extract (3.1 g; yield = 2.1 w*/w*%).

2.5. Preparation of *A. tripedale* Trautv. methanol extract using ultrasonics

The preparation of plant extracts using ultrasonics has proven to be an efficient and effective method. Ultrasonics, based on the potential use of high-frequency sound waves, allows for the extraction of bioactive compounds from plant material through a process known as sonication. This technique enhances the extraction process by breaking down the plant cell walls, releasing the desired compounds into the solvent. The use of ultrasonics also reduces the extraction time and increases the yield, making it a valuable tool for the pharmaceutical, cosmetic, and food industries (Bhaskaracharya et al., 2009; Tang et al., 2023). Additionally, this method is environmentally friendly as it eliminates the need for high temperatures, harsh chemicals, and long extraction time traditionally used in conventional methods (Tang et al., 2023). to subjecting the plant material to ultrasonication, to increase the surface area for extraction, a mixture of 150 g of the stems and leaves of *A. tripedale* Trautv was finely ground and chopped. The pulverized plant sample was then placed into a suitable container or flask capable of withstanding ultrasonic treatment. Then, 200 mL of ultrapure methanol was added to the plant material to completely cover its surface. The ultrasonic energy was directed to the plant sample by creating cavitation bubbles within the solvent. This process enhances extraction by disrupting cell walls and

releasing compounds from the plant material. To prevent the degradation of heat-sensitive compounds, the temperature of the reaction medium was carefully controlled during ultrasonic extraction using a water bath or temperature-controlled ultrasonic equipment. After 15 min., the container was removed from the ultrasonic system. The prepared extract was then filtered to remove any solid particles or plant debris. In the final step, the extract of *A. tripedale* Trautv was concentrated through removing the solvent using rotary evaporation or freeze-drying.

2.6. Antioxidant activity

2.6.1. DPPH assay

To assess the antioxidant activity, a stock solution (1000 mg/mL) was prepared by dissolving 1.0 mg of the plant methanol extract in 1 mL of double distilled water. Further dilutions were made to prepare extract solutions with concentrations ranging from 5-50 µg/mL. Similar concentration ranges were considered for standard samples to enable comparison.

The antioxidant potential of the methanol extracts of *A. tripedale* Trautv. was evaluated using the DPPH assay with slight adjustments. Accordingly, various concentrations of the prepared extract were first mixed with distilled water and a methanolic solution of DPPH (0.1 mM) in brown vials. The mixture was then shaken and kept in darkness at 25 °C for 60 min. to ensure that all the relevant reactions had taken place. The absorbance of each sample was ultimately measured at 517 nm, and the inhibition (%) of the free DPPH radicals or the radical scavenging activity (RSA%) was calculated using the following formula (Eqn. 1):

Inhibition (%) or RSA% = (Ac - As)/Ac (Eqn. 1)

Where Ac and As represent the absorbance of the control and sample, respectively.

The control sample contained all reagents except for the standard or plant extract. The half-maximal inhibitory concentration (IC_{50}), which represents the concentration of each sample needed to inhibit 50% of the free radicals present, was determined by plotting the inhibition (%) as a function of the relevant sample concentrations. The experiments were conducted three times, and the mean inhibitions (%) ± standard deviations (SD) were calculated. Ascorbic acid, gallic acid, and α-tocopherol, as natural antioxidants, were used alongside BHT, a synthetic antioxidant, as positive controls to compare the antioxidant potential of the prepared organic extracts.

2.6.2. Determination of total phenolic content (TPC)

The total phenolic content (TPC) of the MeOH extract prepared from *A. tripedale* Trautv., by the maceration method, was determined using the Folin-Ciocalteu reagent (FCR) based on a previous report (Singleton et al., 1999) with some adjustments. The procedure involved mixing a 0.5 mL aliquot of the sample (either gallic acid (GA) standards at concentrations of 5, 10, 25, 50, 80, and 100 mg/L or the organic extract (tocopherol 500 mg/L) with 0.5 mL of diluted FCR (5.0 *v/v*%) and 1.5 mL of distilled water, and then incubating at 37 °C for 5 min. Next, 1 mL of saturated Na_2CO_3 (10.0 *w/v*%) was added, and the mixture was vigorously shaken for 5 min.. The resulting mixture was left to stand in the dark at room temperature (25 °C) for 2 hours. Finally, the absorbance of each mixture was measured at 760 nm using UV/Vis spectrophotometry against a reagent blank. Gallic acid (GA) was used as a reference phenolic acid, and the TPC was expressed as mg of GA equivalents per gram (mg GAE g^{-1}) of *A. tripedale* Trautv. extract based on the dry weight of the extract using the calibration equation:

$Y = 0.0128X + 0.0352$ ($R^2 = 0.9991$) (Eqn. 2).

2.6.3. Determination of total flavonoids content (TFC)

The MeOH extract of *A. tripedale* Trautv. was analyzed for its total flavonoids content (TFC) using a standard spectrophotometric method (Lamaison and Carnet, 1990) with some adjustments. The method relies on the formation of a stable flavonoid-aluminum complex with a maximum absorption at 415 nm. In this procedure, a 1 mL aliquot of the sample or rutin (Ru) standards (20, 40, 80, 120, and 160 mg/L) was mixed with $AlCl_3$ (10.0 w/w%), CH_3COOK (1.0 M), methanol, and distilled water. After vigorous shaking in the dark for 30 min., the absorbance of each sample was measured at 415 nm. The TFC was then calculated as mg RuE g^{-1} based on the dry weight of *A. tripedale* Trautv. extract using the calibration equation: $Y = 0.008X + 0.2126$ ($R^2 = 0.9945$) (Eqn. 3).

2.6.4. Ferrous ion chelating (FIC) assay using ferrozine

The ferrous ion chelating (FIC) assay using ferrozine serves as an effective assay frequently used in chemistry, biochemistry, and pharmacology, especially in the evaluation of the antioxidant and metal-chelating properties of compounds (Dadashpour et al., 2011). This assay is usually utilized to determine the chelating capacity of compounds towards ferrous (Fe^{2+}) ions. Ferrozine (3-(2-pyridyl)-5,6-diphenyl-1,2,4-triazine-*p*,*p'*-disulfonic acid monosodium salt) is a chemical compound that is capable of forming a stable complex with ferrous ions (Fe^{2+}) (Yeşilyurt et al., 2008). In the presence of a chelating agent that has a higher affinity for ferrous ions than ferrozine, the chelating agent will compete with ferrozine for binding to the ferrous ions. As a result, the formation of the ferrozine-Fe^{2+} complex is inhibited, leading to a decrease in the absorbance of the solution (Anusha et al., 2014; Laksmiani et al., 2016). The concise general procedure to assess FIC of the obtained organic extracts is according to a standard procedure (Mahdavi and Mohammadhosseini, 2022) with slight modifications as follows.

To assess FIC% capacity of the obtained organic extracts, 50 µL of $FeSO_4$ (2 mM) was transferred to a vial containing 1 mL of each *A. tripedale* Trautv extract in methanol (2000 µg/mL) along with 2 mL of distilled water. Subsequently, 100 µL of ferrozine (5 mM) was added to initiate the reaction. The mixture was thoroughly shaken and left to incubate at room temperature for 10 min. The absorbance of each solution was then measured at

562 nm. Each measurement was performed in triplicate while considering such as ethylenediaminetetraacetic acid (EDTA), citric acid (CitA), and ascorbic acid (AscA) positive controls as positive controls. The percentage inhibition of ferrozine-Fe^{2+} complex formation was finally determined using the following formula (Eqn. 4):

$FIC\% = [(A_c - A_s)/A_c] \times 100$ (Eqn. 4)

Where A_c is the absorbance of the control insisted of $FeSO_4$ (50 µL), ferrozine (100 µL), and methanol (1 mL), and A_s accounts for the extract absorbance.

2.7. Antibacterial activity

2.7.1. Microorganisms

The seven studied bacterial strains consisted of three Gram-positive strains, namely *Enterococcus faecalis*, *Staphylococcus coagulase*, *Staphylococcus aureus* along with four Gram-negative strains, namely *Escherichia coli*, *Klebsiella pneumoniae*, *Pseudomonas aeruginosa* and *Proteus vulgaris*.

2.7.2. Disk diffusion approach

The disk diffusion approach is widely used to determine the antibacterial activity of various substances (Adhikari and Rangra, 2023; Dreger et al., 2023). This method involves placing paper disks soaked in a specific substance onto a bacterial culture plate and measuring the zones of inhibitions around the disks (AlAgha et al., 2023). The size of the zone indicates the extent of antibacterial activity exhibited by the substance. This assay is particularly useful in the field of antimicrobial research and development, as it provides a quick and cost-effective way to screen potential candidates for pharmaceutical applications (Rivera et al., 2023). Moreover, the disk diffusion approach allows for the comparison of different substances and their varying degrees of antibacterial efficacy, aiding researchers in identifying the most effective agents for combating bacterial infections (Yerbanga et al., 2023). The general procedure for the performance of the disk diffusion approach is as follows. After loading the suspensions of microorganisms containing 10^8 CFU/mL onto sterile cotton swabs, they were streaked over the dried surface of Mueller-Hinton agar plates for inoculation. The sterile filter paper discs with a diameter of 6 mm were soaked in 20 µL (2 × 10 µL) of each extract (100 mg/mL) and then placed on the agar that had been inoculated. The plates were then incubated at 37 °C for 24 h. The antimicrobial activity was determined through the measurements of the diameter of the zone of inhibition of the disc against the microorganisms. All tests were conducted three times while using chloramphenicol (30 µg) and vancomycin (30 µg) as positive controls and a disc soaked in 20 µL of solvent as the negative control. The extracts of *A. tripedale* Trautv were dissolved in either acetone or methanol using this assay.

2.7.3. Minimum inhibitory concentration (MIC) approach

Antibacterial activity using the minimum inhibitory concentration (MIC) approach is a valuable tool in assessing the effectiveness of antibiotics against different microorganisms (Dalton, 2023). MIC refers to the lowest concentration of a substance that can inhibit the growth of a particular microorganism (Taiyari et al., 2021; Samura et al., 2022). This method allows researchers to determine the smallest amount of an antibiotic needed to prevent bacterial growth, providing important information for future treatment strategies. The MIC approach involves conducting a series of tests where varying concentrations of antibiotics are added to bacterial cultures. The goal is to find the concentration at which the antibiotics completely stop the growth of bacteria. This concentration is considered the MIC (Chaudry and Klausner, 2021; Shi et al., 2021). By determining the MIC, scientists can assess the potency of different antibiotics against specific bacteria. This information can be used to guide the selection of an appropriate antibiotic therapy for a particular infection, ensuring that the most effective treatment is administered to patients. Additionally, the MIC approach can also help researchers investigate the resistance patterns of bacteria, allowing for the development of new antibiotics or the modification of existing ones to combat emerging challenges in antimicrobial therapy (Gupta and Kumar, 2019; Van de Vel et al., 2019; Dalton et al., 2020). Overall, the MIC approach is a crucial tool in the field of antibacterial research, providing valuable insights into the effectiveness of antibiotics and aiding in the development of improved treatment strategies (Van Hal et al., 2012; Kalil et al., 2014; Torres et al., 2015; Bienvenu et al., 2019).

To monitor the minimum inhibitory concentration (MIC) values of the methanol extracts prepared from a combination of the stems and leaves of *A. tripedale* Trautv by the use of three techniques, namely maceration, Soxhlet and ultrasonics, a 96-well plate with 8 rows and 12 columns was used. Using this assay, each well was filled with 100 µL of Mueller-Hinton Broth (MHB) culture medium. The first well contained a 100 µL solution of the extract in DMSO. Serial dilutions of the extract were then made, and 100 µL from each dilution was transferred to consecutive wells. In the next step, 50 µL of MHB and 50 µL of bacteria or fungi inoculum were added to each well. The final volume in each well was 200 µL. The concentrations of the extract ranged from 50 to 0.39 mg/mL, while the concentrations of the positive controls (ampicillin or chloramphenicol) ranged from 100 to 0.78 µg/mL. Each plate was used for only one microorganism. Three wells in the last row were used as growth controls, and three wells were used as negative controls. The plates were covered and incubated at 37 °C for 24 h. The turbidity of each well was then assessed. The MIC was determined as the lowest concentration that showed no visible growth. All the antibacterial tests were performed in triplicate, and the mean value was seen along with the corresponding standard deviation.

2.8. Apparatus

The antioxidant tests were conducted using a UVIKON-922 (Italy) double beam UV/VIS spectrophotometer with matched quartz cuvettes, employing the DPPH assay. The volatile fractions obtained from different parts of

A. tripedale Trautv. were analyzed for their chemical compositions using GC and GC/MS instruments. Gas chromatographic analyses (GCA) were conducted using a Shimadzu 15A GC system equipped with a split/splitless injector and a flame ionization detector (FID) at a temperature of 250 °C. A DB-5 capillary column and ultrapure nitrogen were used as the carrier gas for separation. The oven temperature was programmed to start at 60 °C for 3 min. and then ramped up to 220 °C at a rate of 5 °C/min, holding at this temperature for 5 min.. GC/MS analyses were performed using a Hewlett-Packard 5973 apparatus equipped with an HP-5MS column and a similar temperature program. The MS detector temperature was set at 250 °C, and the corresponding spectra were recorded at an ionization energy of 70 eV (E1) with an electron multiplier voltage of 1800 eV in a mass range of 30-350 amu.

2.9. Headspace solid-phase microextraction (HS-SPME) method

Headspace solid-phase microextraction (HS-SPME) is a technique used in analytical chemistry for the extraction and analysis of volatile and semi-volatile compounds from various matrices. It is especially popular in the fields of environmental, food, fragrance, and forensic analysis (Leszczyńska et al., 2024; Li et al., 2024; Wieczorek et al., 2024; Yin et al., 2024).
The general steps of the performance of this approach are as follows:
i) Sample preparation: The sample, which could be a liquid, solid, or gas, is placed in a sealed container.
ii) Conditioning: In this step, the sample is heated to a specific temperature, allowing volatile compounds to reach equilibrium between the sample and the headspace formed above it.
iii) Fiber selection: A fiber coated with an appropriate stationary phase is selected based on the properties of the compounds being analyzed. The fiber is typically made of silica or other materials and coated with polymers or other sorbent phases.
iv) Extraction: The SPME fiber is inserted into the headspace of the sample container. Volatile compounds partition from the sample matrix into the coating of the SPME fiber due to equilibrium.
v) Desorption: The SPME fiber containing the extracted compounds is then inserted into the injector of a gas chromatograph (GC) or a gas chromatograph-mass spectrometer (GC-MS). The fiber is heated, causing the absorbed compounds to desorb into the GC system for separation and analysis.
In this study, headspace solid-phase microextraction sampling was performed using a manual holder and a 1-cm fused silica fiber tip coated with polydimethylsiloxane and carboxen (PDMS-CAR).
The SPME fiber underwent conditioning following the manufacturer's instructions. For the sampling process, 1.0 g of powdered plant material from different organs of *A. tripedale* Trautv. was first placed into a 20-mL sample vial, sealed with septum-type caps, and heated at 70 °C for 20 min. Subsequently, the PDMS-CAR fiber was positioned outward through the needle, penetrating the septum via the SPME needle, thereby exposing the fiber coating to the headspace above the sample. Following an additional 20 min. of sampling, the fiber was withdrawn into the needle and transferred to the GC/MS injection port. The transfer utilized the splitless mode at a temperature of 250 °C for 5 min.

3. Results and Discussion

3.1. Chemical compositions of the volatile fractions of *A. tripedale* Trautv.

Screening of the chemical profiles relating to the volatile fractions from the concerned organs (flowers, leaves, stems and roots) of *A. tripedale* Trautv. resulted in identification a total of 34, 29, 32, and 33 compounds covering 97.1%, 92.9%, 95.8% and 93.8% of the profile when using the headspace-solid phase microextraction (HS-SPME) approach (see Table 1). Accordingly, the prevailing compounds in the chemical compositions of the volatiles from flowers, leaves, stems and roots of *A. tripedale* Trautv. were diallyl tetrasulfide (15.6%, 23.1%, 25.2%, 20.1%), methyl allicin (18.4%, 13.1%, 21.1%, 15.0%), diallyl thiosulfinate (allicin) (11.2%, 9.1%, 11.1%, 16.0%), and diallyl disulfide (DAS) (8.1%, 3.7%, 7.0%, 12.1%).
In addition, high quantities of vinyl diallyl trisulfide (8.0%) and ethyl diallyl trisulfide (5.3%) were characterized in the volatile fractions obtained from the flowers of *A. tripedale* Trautv. using the HS-SPME-GC/MS approach.

3.2. Frequencies of terpenoids and non-terpenoids in the volatile profiles of different organs of *A. tripedale* Trautv.

The chemical profiles of the different parts of *A. tripedale* Trautv. were characterized by monoterpene hydrocarbons (MH), oxygenated monoterpene (OM), sesquiterpene hydrocarbon (SH), oxygenated sesquiterpene (OS), and non-terpene hydrocarbon (NH) when using the HS-SPME-GC/MS method.
In the HS-SPME profiles of of *A. tripedale* Trautv.:
i) Flowers: Five MHs (3.8%), four OMs (10.1%), two SHs (2.2%), one OS (0.7%), and twenty-two NHs (80.3%) existed with a rank: NH > OM > MH > SH > OS.
ii) Leaves: Two MHs (5.4%), four OMs (5.7%), one SH (1.3%), one OS (16.7%), twenty-one NHs (80.7%) were distinguished representing an order of: NH > OM > MH > SH > OS .
iii) Stems: Four MHs (3.1%), four OMs (2.3%), one SH (1.4%), one OS (0.2%), and twenty-two NHs (88.2%) were present accounting for a total rank: NH > MH > OM > SH > OS.
iv) Roots: Four MHs (3.3%), five OMs (8.6%), two SHs (2.3%), one OS (0.2%), twenty-one NHs (79.4%) representing the following rank: NH > OM > MH > SH > OS.
In Fig. 2, a comparison has been made concerning the relative percentages of the natural compounds groups constituting the chemical profiles of the volatile fractions from different organs of *A. tripedale* Trautv by using the explained HS-SPME-GC/MS method.

Table 1
Chemical compositions of the volatiles from the flowers, leaves and stems of *A. tripedale* Trautv. Karel. using headspace solid phase microextraction (HS-SPME) technique combined with GC/MS.

Sr. Num. [a]	Compound	KI [b]		*Allium tripedale* Trautv. organs			
		Lit. [c]	Cal. [d]	Flowers (%)	Leaves (%)	Stems (%)	Roots (%)
1	α-Pinene	932	931.1	2.1	5	0.9	0.1
2	β-Pinene	974	972.3	1.2	0.4	0.1	0.6
3	1,3-Dithiane	978	978.2	0.1	0.1	-	0.3
4	1-Decene	986	989.1	0.5	0.2	0.2	0.7
5	α-Terpinene	1014	1015.2	-	-	0.7	1.7
6	*p*-Cymene	1020	1022.3	0.1	-	-	-
7	*o*-Cymene	1022	1024.5	0.1	-	-	-
8	1,8-Cineole	1026	1027	-	-	-	0.8
9	Propyl trisulfide	1046	1047.2	1.2	3	0.8	2.7
10	1,3,5-Tritiane	1057	1058.2	0.4	-	0.5	0.1
11	Propenyl trisulfure	1081	1083	-	0.1	-	-
12	γ-Terpinene	1054	1056.1	0.3	-	1.4	0.9
13	*n*-Nonanal	1100	1103.6	0.2	0.4	0.3	0.2
14	Allyl (*E*)-1-propenyl disulfide	1101	1104	0.7	4.1	0.1	-
15	Isopentyl isovalerate	1102	1104.5	-	-	-	1.1
16	Methyl allyl trisulphide	1124	1123.8	1	4.4	-	-
17	Diallyl disulfide (DAS)	1126	1126.2	**8.1**	**3.7**	**7**	**12.1**
18	Allyl propyl disulfide	1131	1130.2	2.1	4.3	3	0.7
19	Methlyl propyl trisulfide	1148	1149.4	0.5	0.1	0.1	0.6
20	Trisulfide	1167	1169.1	0.4	-	1	1.1
21	Diallyl thiosulfinate (Allicin)	1171	1175	**11.2**	**9.1**	**11.1**	**16.0**
22	Methyl allicin	1177	1178.2	**18.4**	**13.1**	**21.1**	**15.0**
23	α-Terpineol	1186	1190.1	2.1	0.2	0.3	-
24	Diallyl trisulfide	1189	1193.1	0.7	1.3	1	0.8
25	Methyl diallyl trisulfide	1192	1195.2	-	0.6	0.1	5.1
26	Ethyl diallyl trisulfide	1203	1202.1	**5.3**	0.1	0.1	0.4
27	Verbenone	1204	1205.6	-	-	-	6
28	1,2-Dithiole	1220	1223.1	0.3	3.5	1.8	-
29	Vinyl diallyl trisulfide	1221	1224.8	**8.0**	**4.4**	**7.1**	0.1
30	Dimethyl trisulfide	1236	1233.7	3.3	1	1.2	0.7
31	1,4-Dimethyl tetrasulfide	1243	1243.2	-	-	0.1	0.9
32	Bornyl acetate	1284	1285.1	0.4	5	1.2	0.2
33	Thymol	1289	1292.1	**7.1**	0.1	0.4	1.3
34	Carvacrol	1298	1299.3	0.5	0.4	0.4	0.3
35	Diallyl tetrasulfide	1338	1337.5	**15.6**	**23.1**	**25.2**	**20.1**
36	Longifolene	1407	1409	0.1	-	-	0.1
37	Germacrene D	1484	1481.3	2.1	1	1.4	2.2
38	14-oxy-α-Muurolene	1767	1764.9	0.7	0.1	0.2	0.2
39	n-Octadecane	1800	1799	1.8	-	0.1	-
40	Hexadecanoic acid	1959	1957.4	0.1	3.3	0.5	0.5
41	l-Eicosene	1987	1989.6	0.4	0.8	**6.4**	0.2
Total				**97.1**	**92.9**	**95.8**	**93.8**
Monoterpene hydrocarons (MHs) percentage				3.8	5.4	3.1	3.3
Oxygenated monoterpenes (OMs) percentage				10.1	5.7	2.3	8.6
Sesquiterpene hydrocarons (SHs) percentage				2.2	1	1.4	2.3
Oxygenated sesquiterpenes (OSs) percentage				0.7	0.1	0.2	0.2
Non-terpene hydrocarons (NHs) percentage				**80.3**	**80.7**	**88.8**	**79.4**

[a] Sr. Num.: Serial number, [b] KI: Kovats index, [c] Lit.: Literature, [d] Cal.: Calculated

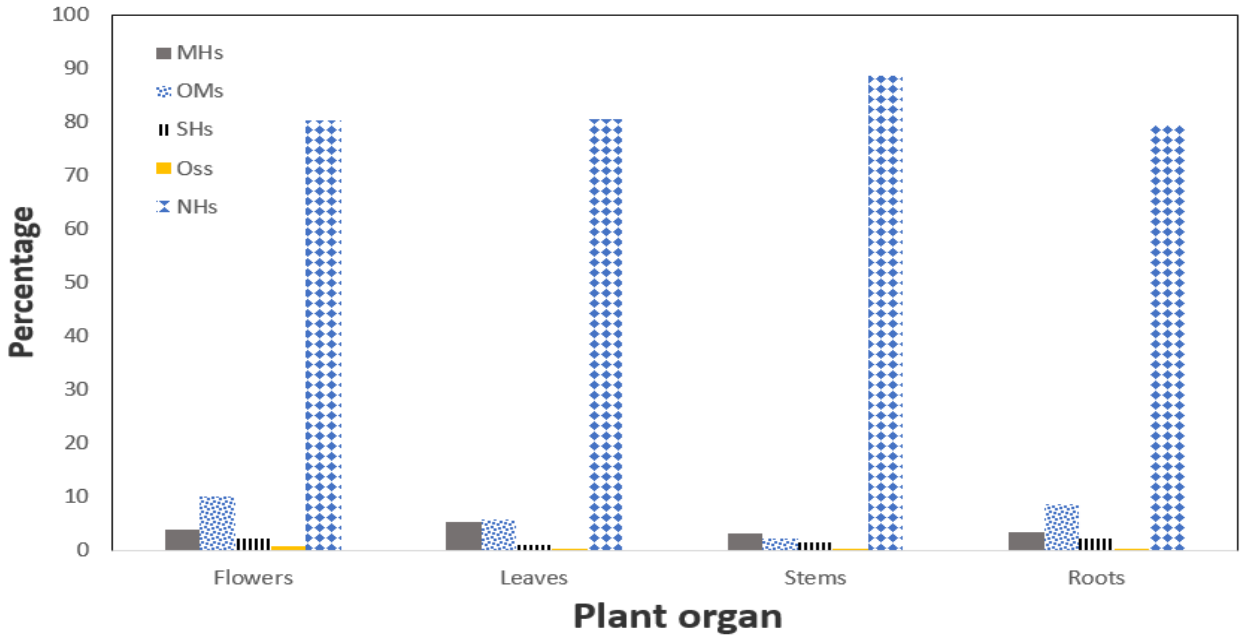

Fig. 2. Comparison of the total percentage of different classes of natural compounds constituting groups of the volatile fractions from flowers, leaves, stems and roots of *A. tripedale* Trautv. using headspace-solid phase microextraction combined with GC/MS (HS-SPME-GC/MS) approach.

3.3. The literature background concerning thse screening of diverse *Allium* species using SPME approach

A simple literature survey demonstrates that some authors have analyzed different species of the *Allium* genus within the past few decades. In this relation, a commercially available SPME-HPLC interface has been employed for the quantitative and qualitative analysis of *Allium* volatiles (Jaillais et al., 1999). As per this investigation, volatiles captured using liquid nitrogen were initially moved to reverse phase-high performance liquid chromatography (RP-HPLC) through a traditional injection method. This study compares outcomes derived from the conventional injection technique with those from SPME utilized in headspace mode. Based on the emphasis and findings of this study, the proposed interface may be utilized when preserving the sample is crucial, although thiosulfinates experience partial degradation.

Kim et al. (2011) have evaluated volatile distribution of *A. sativum* L. using SPME technique under diverse processing conditions. In accordance with this study, the total peak areas observed in crushed-raw garlic were the highest, while those in aged-black garlic clove were the lowest. The effects of crushing were clearly noticeable in raw garlic, aged-black garlic, and roasted garlic cooked at 200°C for 60 min.. Sulfur-containing volatiles, such as diallyl disulfide and diallyl trisulfide, were identified as the major constituent and prevailing components. As being reported, the peak areas of diallyl disulfide generally decreased after garlic underwent autoclaving and roasting, whereas diallyl trisulfide and allyl methyl trisulfide increased during heat treatment compared to raw garlic. This report revealed that roasting at 200 °C for 60 min. notably led to the formation of pyrazines in garlic. Moreover, the principal component analysis (PCA) conducted on the volatile profiles using SPME-GC/MS effectively distinguished between different types of processed garlic.

In another study, the authors have utilized HS-SPME-GC-MS to identify the volatile profiles consisting of organic compounds present in both onion and shallot (D'Auria and Racioppi, 2017). In this report, the primary constituents included dipropyldisulphide and allylpropyldisulphide. Thiopropanal S-oxide was exclusively detected in onion volatiles. Notably, the presence of 2-methyl-2-pentenal, a compound known for its strong fruity aroma, in shallot is noteworthy as it contributes to the distinctive aroma disparity between onion and shallot. Furthermore, SPME-GC-MS analysis of shallot, following absorption on the SPME fiber at 50 °C, revealed the presence of new compounds, the structures of which were deliberated upon.

Using the HS-SPME technique combined GC/MS with, Biancolillo et al. (2022) were able to successfully identify the relevant chemical profiles of sixty-eight samples of red garlic harvested in four distinct Italian regions. In this report, a proper Box-Behnken design was taken into consideration for the optimization of the experimental conditions. In addition, following the collection of GC-MS signals and the identification of volatiles, the authors attempted geographical classification using partial least squares discriminant analysis (PLS-DA). Furthermore, for the external validation, the studied samples were classified into the training (42) and test (26) sets. The PLS-DA model accurately classified 21 external samples. Eventually, variable importance in projection (VIP) analysis pinpointed 13 organosulfur compounds, viz., two sulphides, eight disulphides, and three trisulphides out of the 25 detected constituents, highlighting a

garlic flavor content significantly influenced by the geographical origin of the bulbs.

In the recent report of Xie et al. (2022) on volatile characterized compounds of *A. tuberosum* Rottler or Chinese chive, a total of 59 volatile compounds have been successfully identified using an optimized method. The characterized compounds belong to different organic groups with dimethyl trisulfide (10,623.30 μg/kg) as the most abundant component. By calculating the odor activity values (OAVs), 11 volatile compounds were identified as the major aroma-active compounds of Chinese chive. From the analysis of the composition of Chinese chive aroma, the "garlic and onion" odor (OAV = 2361.09) showed an absolute predominance over the other 5 categories of aroma. The results of this study elucidated the main sources of Chinese chive aroma from a chemical point of view and provided the theoretical basis for improving the flavor quality of Chinese chive.

Volatile profiling of *Allium tenuissimum* L. flower fried by four different oils (rapeseed, peanut, soybean and sunflower), using SPME-GC-MS and gas chromatography-olfactometry (GC-O) as well as sensory evaluation in combination with partial least squares regression (PLSR) has been recently reported (Zhang et al., 2022a). Accordingly, a total of fifty volatile compounds were detected, comprising eight sulfur-containing compounds, ten nitrogen-containing heterocyclics, seven oxygen-containing heterocycles, eleven aldehydes, six acids, and eight other compounds. Through sensory evaluation, onion, caramel, grassy, fatty, and roasty attributes received the highest scores. PLSR analysis elucidated positive correlations between sensory attributes and aroma-active compounds. Specifically, PLSR revealed that the 'roasted' attribute was positively associated with methylpyrazine, 2,5-dimethylpyrazine, and 2,3-dihydro-3,5-dihydroxy-6-methyl-4H-pyran-4-one. The 'onion' attribute showed significant positive associations with dimethyl disulfide and dimethyl trisulfide. 2-Pentylfuran, furfural, and 2-furanmethanol had a notable positive impact on the 'caramel' attribute. Additionally, (*E*)-2-heptenal and (*E*,*E*)-2,4-heptadienal were positively linked to the 'grassy' attribute, while the 'fatty' attribute exhibited significant positive correlations with (*E*,*E*)-2,4-nonadienal, (*E*,*E*)-2,4-decadienal, and heptanoic acid.

3.4. Antioxidant activity results

3.4.1. Results of half-maximal inhibitory concentration (IC_{50}) of the methanol extracts of *A. tripedale* Trautv

Using the DPPH assay and according to the aforementioned procedure, the radical scavenging activity (RSA%) of the achieved organic extracts obtained by the use of maceration, Soxhlet and ultrasonic methods was first calculated. Then, after plotting the percentage inhibition against the log concentration of the organic extract, a dose-response curve was obtained which was further used to determine the concentration of the organic extract that inhibits about 50% of the free DPPH radical (IC_{50}) through the interpolation or curve fitting methods (see Table 2).

To ensure reproducibility of the results, each assay was permitted to be done for three replicates and the mean results were used for the construction of RSA% plot. According to the results tabulated in Table 2, the extracts obtained by maceration, and ultrasonic techniques for a mixture of the stems and the leaves of *A. tripedale* Trautv resembled excellent IC_{50} values of 5.36 ± 0.69, 33.27 ± 1.23 and 11.01 ± 0.56 comparable to those obtained for the vitamin E and BHT as the standards. More importantly, the extracts of the plant material prepared by the use of maceration and ultrasonic displayed lower IC_{50} values than the employed standards (Vitamin E and BHT) confirming their higher antioxidant power. A literature survey demonstrates that no report could be found dealing with the antioxidant activity of the essential oil or organic extracts of *A. tripedale* Trautv.

3.4.2 Quantification of the of total phenolic content (TPC)

The amount of total phenolic content (TPC) of the methanolic extracts prepared from a mixture of the stems and the leaves of *Allium tripedale* Trautv. was calculated based on the absorption values resulting from the reaction of the extract with Folin-Ciocalteu reagent (FCR) aqueous reagent compared to those of gallic acid standard solutions according to the equation of the line obtained from the gallic acid standard curve ($y = 0.0322x + 0.0354$, $R^2 = 0.9567$). In view of the obtained results for the evaluation of the TPC (see Table 2), it was noted that there was not a considerable difference between the TPC for the organic extracts using maceration, Soxhlet and ultrasonic techniques. In this relation, the following rank was concluded in terms of mg RuE g^{-1}: Maceration (15.41) > Ultrasonic (12.23) > Soxhelt (8.18).

3.4.3. Determination of the total flavonoid content (TFC)

The amount of total flavonoid content (TFC) of the methanolic extracts from a mixture of the leaf + stem of *A. tripedale* Trautv. was calculated by aluminum chloride colorimetric method, based on comparison with rutin standard solutions and according to the linear equation of the relevant standard curve ($y = 0.0093x + 0.0906$, $R^2 = 0.9586$). According to the tabulated results in Table 2, for a mixture of the stems and the leaves of *A. tripedale* Trautv using the employed maceration, Soxhlet and ultrasonic approaches, the calculated TFC represented the following rank in terms of mg GAE g^{-1}: Maceration (139.0) > Ultrasonic (53.76) > Soxhelt (30.107).

3.4.5. Determination of ferrous ion chelating (FIC)

Lipid oxidation is a significant contributor to the oxidative degradation of low-density lipoprotein (LDL) and the deterioration of food products (Ayala et al., 2014; Mozuraityte et al., 2016; Kiokias et al., 2018). This process could be performed via radical chain reactions, typically initiated by transition metal ions like iron and copper, which are common initiators in both biological systems and food stuff (Antolovich et al., 2002). Consequently, the metal chelating ability of

Table 2
Total phenolic content (TPC) and total flavonoid content (TFC), inhibitory activity (IC_{50}) using DPPH assay of the methanolic extract from a mixture of the stems and the leaves of *Allium tripedale* Trautv maceration, Soxhlet and ultrasonic approaches.

Extraction process	TPC (mg GAE g^{-1})	TFC (mg RuE g^{-1})	Half-maximal inhibitory concentration (IC_{50}) (µg/mL)	Ferrous ion chelating (FIC%)
Maceration	15.41±0.93*	139.0±1.9*	5.36±0.69*	8.2±1.5*
Soxhelt	8.18±0.37*	30.107±2.87*	33.27±1.23*	74.0±5.24*
Ultrasonic waves	12.23±0.72*	53.76±0.38*	11.01±0.56*	80.9±s1.40*
Vitamin E	-	-	55.81±0.98*	-
BHT	-	-	17.08±0.465*	-
Ascorbic acid	-	-	-	1426.64±67.43*
Citric acid	-	-	-	1446.78±88.25*
Ethylenediaminetetraacetic acid (EDTA)	-	-	-	67.23±5.21*

GA: Gallic acid; Ru: Rutin *Values are presented as means ± SD (n = 3), BHT: Butylated hydroxytoluene

other compounds, such as synthetic antioxidants or plant extracts, may inhibit lipid oxidation through the chemical process of complex formation with metal ions. Ferrozine is widely recognized as a reagent that forms a stable complex with ferrous ions in a quantitative manner due to its high sensitivity and low cost. When the other chelating agents exist in the reaction medium, the ferrozine-iron complex is disrupted, resulting in the fading of the complex color (purple). The FIC% calculated for the methanol extract of a mixture of the stems and the leaves of *A. Tripedale* Trautv. yielded by maceration, was found to be very low (8.2 ± 1.5%) (see Table 2). However, under the same circumstances, the FIC% for the other two organic extracts (Soxhelt and ultrasonic) were found to be remarkably higher being 74 ± 5.24 and 80.9 ± 1.40%. Nevertheless, all the calculated FIC% for all the prepared extracts were remarkably lower than those observed for ascorbic acid (1426.64 ± 67.43%) and citric acid (1446.78 ± 88.25%) and comparable to that of EDTA (67.23 ± 5.21%).

3.5. Antibacterial results

3.5.1. Disk diffusion results

According to the tabulated results in Table 3, the highest antibacterial activity using the disk diffusion method and the highest inhibition zone diameter (IZD) for the methanolic extract obtained from a mixture of the stems and the leaves of *Allium tripedale* Trautv using maceration technique was observed against *E. faecalis*. Using Soxhlet technique, the highest IZD for the aforementioned organic extracts was seen against *E. coli*. The organic extracts obtained by ultrasonic showed the best antibacterial activity against *E. faecalis* with an IZD of 9.0 ± 0.1 (mm). A perusal of this table also shows that the lowest antibacterial activity and the least IZDs were found against *S. aureus* (7.6 ± 0.2), *S. aureus* (7.4 ± 0.2 mm) and *E. coli* (7.0 ± 0.1 mm) for the methanol extracts prepared by maceration, Soxhlet and ultrasonic techniques. Furthermore, regarding the numerical values of IZD for the studied bacterial strains, it was realized that *K. pneumonioae* and *P. aeruginosa* bacteria represented the same antibacterial activity for all the extracts. On the other hand, the highest antibacterial acuity for the standards were noted for vancomycin against *E. faecalis* (17.3 ± 0.6 mm) and *S. coagulase* (17.2 ± 0.3 mm). It should also be noted that, in comparison to the standard antibiotic vancomycin, higher IZDs were observed in most cases for chloramphenicol compared to the other bacteria studied. In this sense, the optimal numerical values of IZDs (mm) were 26.3 ± 0.6 *vs. E. faecalis*, 25.3 ± 0.3 *vs. E. coli*, 23.5 ± 0.5 *vs. K. pneumonioae*, 23.2 ± 0.3 *vs. S. aureus* and 20.3 ± 0.6 *vs. P. vulgaris*.

3.5.2. Minimum inhibitory concentration (MIC) results

To examine the relevant antibacterial activity, using MIC assay (µg/mL), for methanolic extracts from a mixture of the stems and the leaves of *A. tripedale* Trautv using maceration, Soxhlet and ultrasonic approaches, the detailed procedure in subsection 2.7.3. was followed. Surprisingly, in most of the cases, the same MIC (250 µg/mL) (Table 4) was obtained. However, the ultrasonic extracts were found to be insensitive against *E. coli* and *P. vulgaris*. Additionally, among the three organic extracts against *S. aureus*, only the ultrasonic one demonstrated moderate to weak MIC (250 µg/mL). Furthermore, under the same optimized conditions, all the antibiotic standards used displayed the same antibacterial activity with an MIC of 25 µg/mL. Although antibacterial activity of the some essential oils (Najafi et al., 2016; Ortega-Ramirez et al., 2016; Zabihi et al.,

Table 3
The antibacterial results for methanolic extracts from a mixture of the stems and the leaves of *Allium tripedale* Trautv using maceration, Soxhlet and ultrasonic approaches by disc diffusion method (mm).

Standard (Chl.)	Standard (Van.)	Ultrasonic	Soxhlet	Maceration	Bacterial strain
0.3±25.3	0.3±8.2	0.1±7.0	0.3±9.2	0.3±8.2	*E. coli*
0.5±23.5	0.3±7.8	0.2±8.0	0.1±8.0	0.1±8.0	*K. pneumonioae*
-	-	0.2±8.0	0.1±8.0	0.2±8.0	*P. aeruginosa*
0.6±20.3	0.3±6.0	0.3±7.2	0.3±8.3	0.2±8.4	*P. vulgaris*
0.6±26.3	0.6±17.3	0.1±9.0	0.1±8.0	0.1±9.0	*E. faecalis*
0.3±7.7	0.3±17.2	0.1±8.0	0.3±8.6	0.3±8.3	*S. coagulase*
0.3±23.2	0.3±14.3	0.2±7.2	0.3±7.4	0.2±7.6	*S. aureus*

Van: Vancomycin; Chl.: Chloramphenicol

Table 4
Antibacterial MIC test results (µg/mL) for methanolic extracts from a mixture of the stems and the leaves of *Allium tripedale* Trautv using maceration, Soxhlet and ultrasonic approaches.

Bacterial strain	Extraction process		Standards		
	Maceration	Soxhlet	Maceration	Chl.	Amp.
E. coli	250	250	250	25	25
K. pneumonioae	250	250	250	25	25
P. aeruginosa	250	250	250	25	25
P. vulgaris	250	250	250	25	25
E. faecalis	250	250	250	25	25
S. coagulase	250	250	250	25	25
S. aureus	-	-	-	25	25

Amp.: Ampicillin; Chl.: Chloramphenicol

2017; Ebadi et al., 2022) or extracts (Stan et al., 2016; Otunola et al., 2017; Nnamchi et al., 2021; Al-Kubeisi, 2022; Ourouadi et al., 2022) of some *Allium* species has been the subject of some reports in the literature, to the best of our knowledge, this is the first report dealing with the antibacterial activity of *A. tripedale* Trautv. extracts.

3.6. Response surface methodology (RSM) modeling using central composite design (CCD) approach

To choose the best experimental conditions for the performance of the proposed approaches, a rotatable and orthogonal central composite design (R&O-CCD) was used. Accordingly, for all the relevant points, the corresponding variance for the calculated response was considered to be the same and constant for all the points having the same distance from the design center. In this relation, if each experimental variable is evaluated independently, the corresponding experimental design will be orthogonal. This specific type of geometry allows us to evaluate the main impacts of the affecting experimental variables as well as their potential interactions along with quadratic influences.
This design typically consists of a half-fraction factorial design in which:

$N_f = 2^{f-1}$ (Eqn. 5)

While the term F denotes the number of factors. A star design also exists for which:

$N_\alpha = 2f$ (Eqn. 6)

Furthermore, some repeated experiments are preferably recommended to be done at the centeral levels of the relevant factors (N_0). As it is customary in these types of simulations, the experiments would be repeated multiple times at the central points to achieve a better (lower) experimental error. Moreover, the axial points were adjusted at an interval of -α to +α from the central part of the experimental values. According to the literature, the optimized value for the term α to achieve R&O-CCD would be equal to ±1.682 using the following formula (Eqn. 7):

$á = \sqrt[4]{N}$ (Eqn. 7)

For the construction of the model and evaluation of the chosen experimental variables, analysis of variance (ANOVA) was taken into consideration in which the numerical F-value accounts for the importance of the proposed model (Morgan, 1991; Zeaiter et al., 2004).

3.6.1. RSM: CCD for the solid phase microextraction

(SPME) process

The variables used for the SPME technique were A: Temperature (ºC), B: Time (min.) and C: Quantity (g). To carry out a comprehensive experimental design, the software "Design-Expert" (Version 13) was used again. The details for the runs, experimental variables, the obtained responses as well as the statistical results of ANOVA approach have been tabulated in Table 5. Using the statistical ANOVA, the following equation (Eqn. 8) was obtained:

$R = 15.38 + 0.1862A + 0.1188B + 0.0411C + 0.0188AB - 0.0062AC + 0.0062BC - 0.1193A^2 - 0.0574B^2 - 0.0132C^2$ (Eqn. 8)

Where the terms R, A, B and C, respectively account for the relative percentage of the most abundant constituent component of SPME (response factor), temperature (ºC), time (min.) and quantity (g). According to the tabulated data in Table 6, the F-value of the proposed quadratic model (132.83) implies the model is significant. In fact, in this model, there is only a 0.01% chance that an F-value could occur due to noise. Additionally, *p*-values less than 0.0500 indicate that some model terms involving A, B, A^2, B^2 are significant, while the other terms are considered to have insignificant impacts. The lack of fit F-value of 1.44 implies the it is not significant relative to the pure error. There is a 34.81% chance that a lack of fit F-value could occur due to noise. Once again, it is apparent that non-significant lack of fit is preferred in statistical-based evaluations.

However, to obtain a better model in which all of the implemented terms have significant impacts, model construction was performed again using model reduction and the following equation (Eqn. 9) was obtained.

$R = 15.38 + 0.1862A + 0.1188B + 0.0711C + 0.0188AB - 0.1193A^2 - 0.0574B^2 - 0.0132C^2$ (Model F-value = 190.22) (Eqn. 9)

The statistical features and fit statistics obtained for the ANOVA of the new proposed quadratic model have been summarized in Table 7. A simple comparison between the numerical values of the term predicted R^2 before and after the implementation of model reduction approach (0.9691 *vs* 0.9576) represents the higher predictability of the reconstructed model.

Using the Design-Expert software for the proper experimental design of our developed HS-SPME approach, a number of plots and tables were obtained. In accordance with the potential use of this software:

i) The normal percentage probability as a function of externally studentized residuals for the SPME technique has been shown in Fig. 3. This plot is a graphical tool used to check several assumptions of linear regression consisting of:

a) Homoscedasticity: This plot helps to assess whether the variance of the residuals is constant across different levels of the predicted values. A horizontal band of points with constant spread indicates homoscedasticity, while a cone-shaped or funnel-shaped pattern may indicate heteroscedasticity (non-constant variance).

b) Linearity: It helps to assess whether the relationship between the dependent variable and the independent variables is linear. A roughly random scatter of points around zero suggests linearity.

c) Outliers and influential points: Points that deviate substantially from the overall pattern may indicate outliers or influential points that have a disproportionate impact on the regression results. As can be seen in Fig. 3, there is no outlier in our developed model and the general trend observed seems to be rational (Rofouei et al., 2021).

ii) The Box-Cox plot for power transforms for the SPME technique has been tabulated in Fig. 4. The Box-Cox plot is a graphical tool used in statistics to help identify an appropriate power transformation for data that exhibits heteroscedasticity (varying levels of spread) or non-normality and helps in visually identifying the lambda value that best transforms the data to meet the assumptions of normality and homoscedasticity (constant variance) required by many statistical techniques, thus making the data more amenable to analysis using those techniques (Biscay Lirio et al., 1989; Atkinson et al., 2021).

The plot is used to determine the optimal value of lambda (λ) in the Box-Cox transformation, which is a family of power transformations defined as Eqn. 10:

$$y_{(\lambda)} = \begin{cases} \frac{y^{\lambda}-1}{\lambda}, & \text{if } \lambda \neq 0 \\ \ln(y), & \text{if } \lambda = 0 \end{cases}$$ (Eqn. 10)

In the context of the Box-Cox transformation and the associated plot, lambda (λ) represents the power parameter that is applied to the data during transformation. Lambda can take any real value, except for zero (0). When lambda equals zero, the transformation simplifies to a logarithmic transformation. The purpose of lambda in the Box-Cox transformation is to find the best power transformation to stabilize the variance and make the data distribution more approximately normal. By varying lambda, different transformations of the data can be explored. A lambda of 1 corresponds to no transformation, and as lambda moves away from 1 (either towards 0 for a logarithmic transformation or away from 0), it applies different degrees of power to the data (Chagas et al., 2019; Obradović et al., 2020).

The Box-Cox transformation aims to stabilize the variance and/or make the data more approximately normally distributed.

To calculate the Box-Cox transformed values, for a given range of lambda values (typically ranging from -2 to 2), the Box-Cox transformation is applied to the original data.

The transformed data's normal quantile plot (Q-Q plot) or some other diagnostic plot (such as scatter plot of transformed data against original data) is plotted against the lambda values.

The lambda value that results in the most linear or symmetric plot (such as the one closest to a straight line for Q-Q plot or the one that appears to have stabilized variance) is selected as the optimal lambda for the Box-Cox transformation (lambda = 3, see Fig. 4). However, in our modeling using Design-Expert software, no transform was recommended while considering lambda = 3 (current lambda).

iii) The schematic representation of the trends of externally studentized residuals as a function of the predicted values for the SPME can be seen in Fig. 5. This trend usually refers to a diagnostic plot commonly

used in regression analysis to assess the assumptions and validity of the regression model. By examining this plot, analysts can identify potential issues with the regression model and take appropriate corrective actions, such as transforming variables, using robust regression techniques, or identifying and addressing influential data points (Gangaram et al., 2014; Zhang et al., 2022b).

In this approach, the concerned residuals account for the differences between the observed values of the dependent variable and the values predicted by the regression model. In fact, externally studentized residuals are a type of standardized residuals that adjust for the potential influence of each observation on the estimation of the model parameters. These terms are typically referred to as "externally studentized" because they are standardized using an estimate of the error variance that excludes the effect of the observation being assessed. In addition, the predicted values represent the values of the dependent variable forecasted by the regression model based on the independent variables.

iv) Fig. 6 represents the Cook's distance as a function of run numbers for the SPME technique. In Design-Expert software, "Cook's distance as a function of run numbers" refers to a diagnostic plot used in regression analysis, particularly in the context of design of experiments (DOE) (Takahashi, 2022). Cook's distance stands for a measure that helps assess the influence of individual data points on the overall regression model. It quantifies how much the regression coefficients would change if the model were fitted without that particular data point. In other words, Cook's distance helps identify observations that have a disproportionate impact on the regression results. By examining this plot, analysts can decide whether to remove or downweight influential points, investigate potential sources of variability, or consider alternative modeling approaches. It helps ensure the reliability and robustness of the regression model and the conclusions drawn from the analysis (Martín and Pardo, 2009; Martín, 2015; Pinho et al., 2015; Kim, 2017). On the other hand, in Design-Expert software, "run numbers" typically refer to the sequence or order in which experiments or runs were conducted in a designed experiment. Each run number corresponds to a specific combination of factor levels or settings.

The plot of Cook's distance as a function of run numbers (Fig. 6) helps analysts identify influential data points or runs in the experiment. Points with high Cook's distance are considered influential, meaning they have a significant impact on the regression model. These points may represent outliers, data entry errors, or instances where the model assumptions are violated. As seen in this figure, all the relevant points fall within the logical range confirming the appropriateness of the suggested model.

v) The two dimensional contour plot representing the interactions of the terms A: Temperature and B: Time for the SPME has been represented in Fig. 7. In Design-Expert software, a two dimensional contour plot is a graphical representation used to visualize the relationship between multiple variables (dimensions) and the response (output) of a process or system. Two dimensional contour plots are powerful visualization tools that help researchers and engineers understand complex relationships between variables and responses, identify optimal process settings, and make informed decisions to improve product or process performance. These plots are particularly useful in design of experiments (DOE) and response surface methodology (RSM) for understanding how changes in input variables affect the output response. The key components of a dimensional contour plot typically represent involve:

1) Dimensions or variables: These are the independent variables or factors that are under investigation or control in the experiment. They could represent factors like temperature, pressure, concentration, time, etc.

2) Response: This is the dependent variable or output that is being observed or measured in response to changes in the independent variables. It could represent product yield, reaction rate, tensile strength, etc.

3) Contour lines: Contour lines on the plot connect points that have the same response value. Each contour line represents a specific level of the response variable. By observing the contour lines, one can understand how changes in the input variables affect the response (Dias et al., 2021; Pandey and Sara, 2023). According to the Fig. 7, for the most influential parameters in our proposed SPME approach involving temperature and time and specific amount of plant material, an enhancement of time causes to reach the optimal response. This behavior is also observed by an increase of time. So, the optimized amount of time and temperature to get the best results were found to be Time = 60 min (in the conditioning step) and Temperature = 80 °C.

4) Interaction effects: Dimensional contour plots may also show how interactions between different variables influence the response. For example, the contour lines may change direction or shape, indicating that the effect of one variable on the response depends on the level of another variable.

Optimization: Design-Expert software often allows users to perform optimization based on the contour plots. Users can identify regions of interest where the response is maximized or minimized, and the software can suggest optimal settings for the input variables to achieve desired outcomes.

vi) The 3D surface plot representing the interactions of the terms A: Temperature and B: Time for the SPME has been represented in Fig. 8. According to the Fig. 8, at a constant temperature, the main response first increases and then drops with the increase of time and the same trend is seen at the constant time when the temperature increases. However, the factor temperature is considered to be more influential rather than the time.

vii) Finally, the disturbtion plot for the trends of variation of the three experimental variables has been displayed in Fig. 9. The perturbation plot helps researchers to compare the effects of all the factors at a particular point in the design space. This plot is often drawn by monitoring the general change of only one factor over its range while holding all the other factors constant. As can be seen from the relevant perturbation plot (see Fig. 8) all the experimental factors exert a positive impact on the response factor. However, the general influences of these parameters are according to the following order: Temperature > Time > Plant quantity.

Table 5
Runs, experimental variables, general details of the experimental design approach and the obtained responses being fed to Design-Expert software for the solid phase microextraction (SPME) approach.

Std	Run	Factor 1	Factor 2	Factor 3	Response 1
		A:Temperature C	B:Time Min.	C:Quantity g	R1
9	1	53.182	45	0.75	14.7
20	2	70	45	0.75	15.35
4	3	80	60	0.5	15.45
13	4	70	45	0.330	15.2
7	5	60	60	1	15.2
14	6	70	45	1.170	15.45
12	7	70	70.227	0.75	15.4
19	8	70	45	0.75	15.4
3	9	60	60	0.5	15.05
1	10	60	30	0.5	14.85
6	11	80	30	1	15.3
8	12	80	60	1	15.6
11	13	70	19.773	0.75	15
5	14	60	30	1	15
2	15	80	30	0.5	15.2
16	16	70	45	0.75	15.4
10	17	86.818	45	0.75	15.35
18	18	70	45	0.75	15.4
17	19	70	45	0.75	15.4
15	20	70	45	0.75	15.35

Table 6
The ranges of the changes of the experimental variables affecting the solid phase microextraction (SPME) technique.

Variable	SPME				
	-α	-1	0	1	+α
A: Temperature (°C)	53.2	50	70	80	86.8
B: Time (min.)	19.8	30	45	60	70.2
C: Quantity (g)	0.33	0.5	0.75	1	1.2

Table 7
The statistical results of ANOVA approach on the suggested new quadratic model regarding model reduction approach for the SPME technique by Design-Expert software.

Source	Sum of Squares	df	Mean Square	F-value	*p*-value	
Model	0.974	7	0.139	190.22	< 0.0001	significant
A-Temperature	0.474	1	0.474	647.71	< 0.0001	
B-Time	0.193	1	0.193	263.7	< 0.0001	
C-Quantity	0.069	1	0.069	94.31	< 0.0001	
AB	0.003	1	0.003	3.85	0.074	
A^2	0.205	1	0.205	280.49	< 0.0001	
B^2	0.048	1	0.048	64.99	< 0.0001	
C^2	0.003	1	0.003	3.45	0.088	
Residual	0.009	12	0.001			
Lack of Fit	0.005	7	0.001	1.17	0.448	not significant
Pure Error	0.003	5	0.001			
Cor Total	0.982	19				
Std. Dev.	0.027					
Mean	15.25					
C.V. %	0.177					
R^2	0.991					
Adjusted R^2	0.986					
Predicted R^2	0.969					
Adeq Precision	50.024					

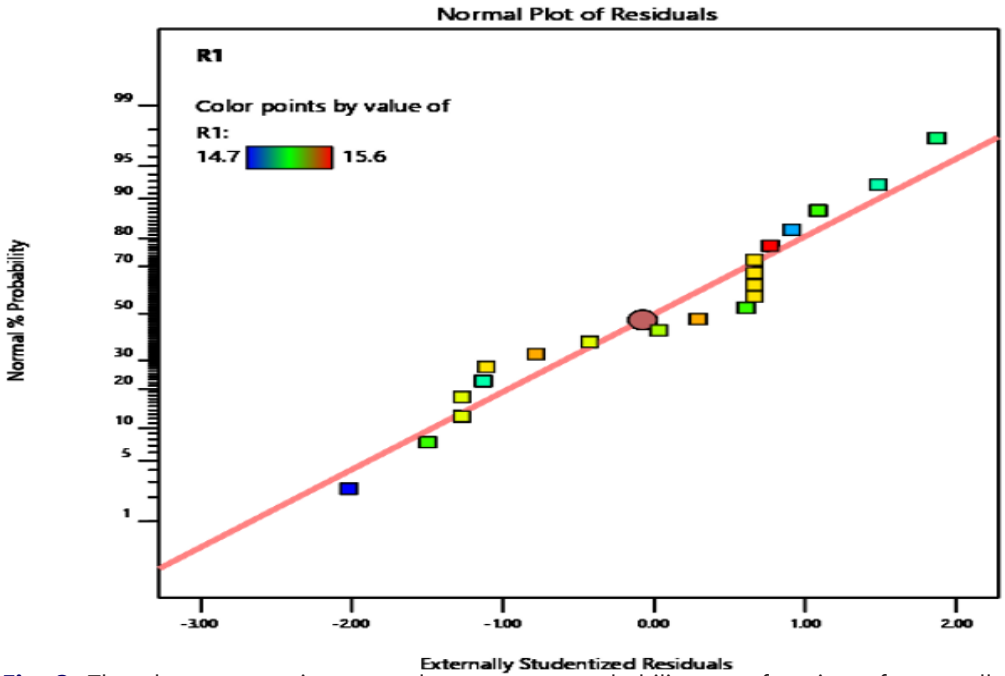

Fig. 3. The plot representing normal percentage probability as a function of externally studentized residuals for the SPME technique (after exerting model reduction approach).

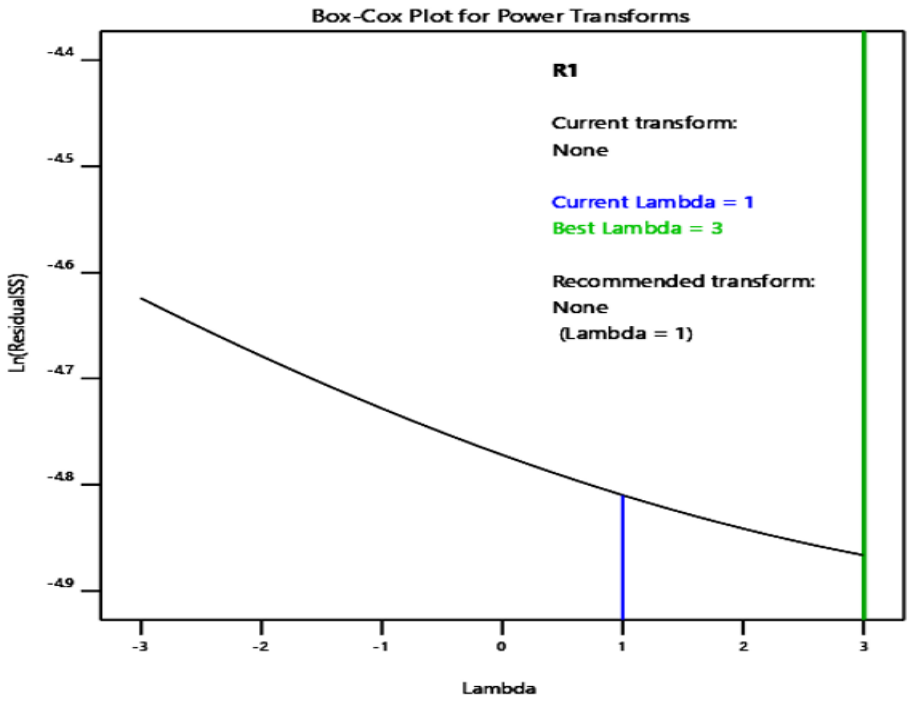

Fig. 4. The Box-Cox plot for power transforms for the SPME technique using Design-Expert software (after exerting model reduction approach).

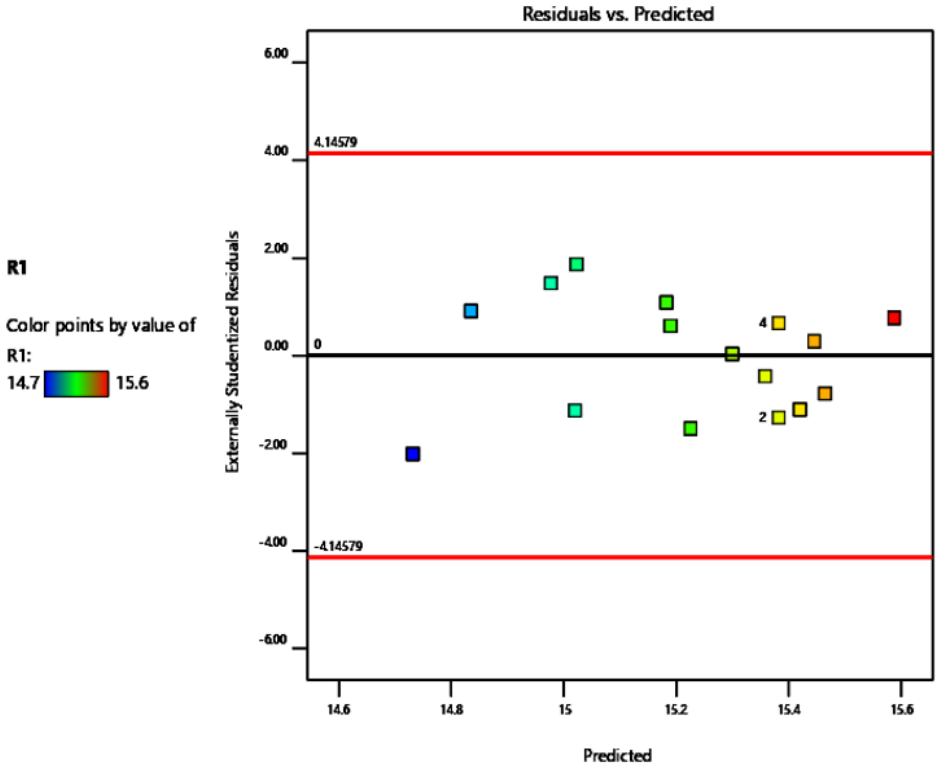

Fig. 5. The schematic representation of the trends of externally studentized residuals as a function of the predicted values for the SPME technique using Design-Expert software (after exerting model reduction approach).

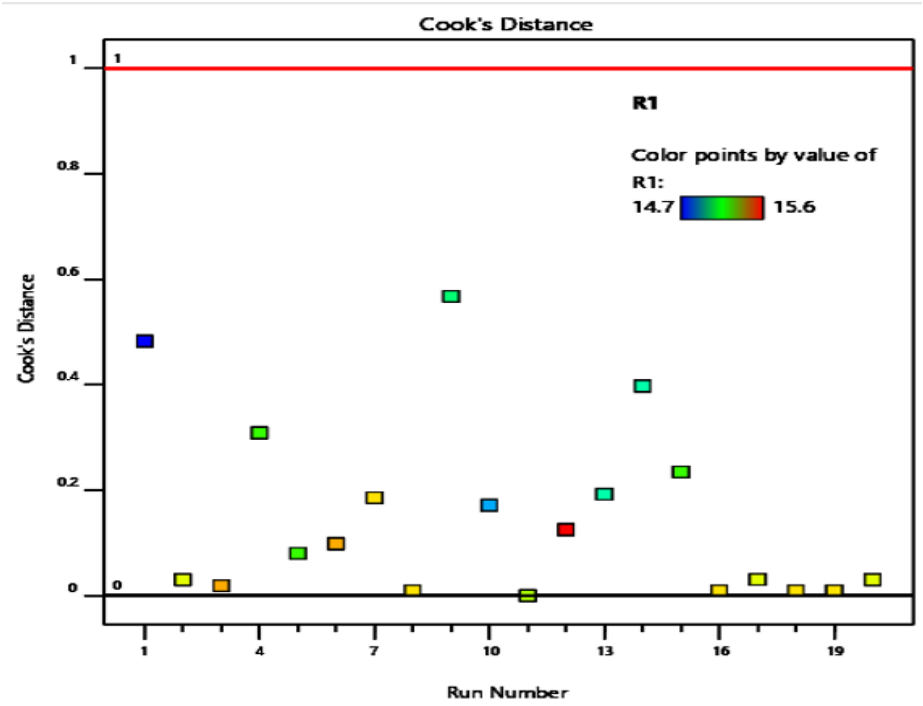

Fig. 6. The schematic representation of Cook's distance as a function of run numbers for the SPME technique using Design-Expert software (after exerting model reduction approach).

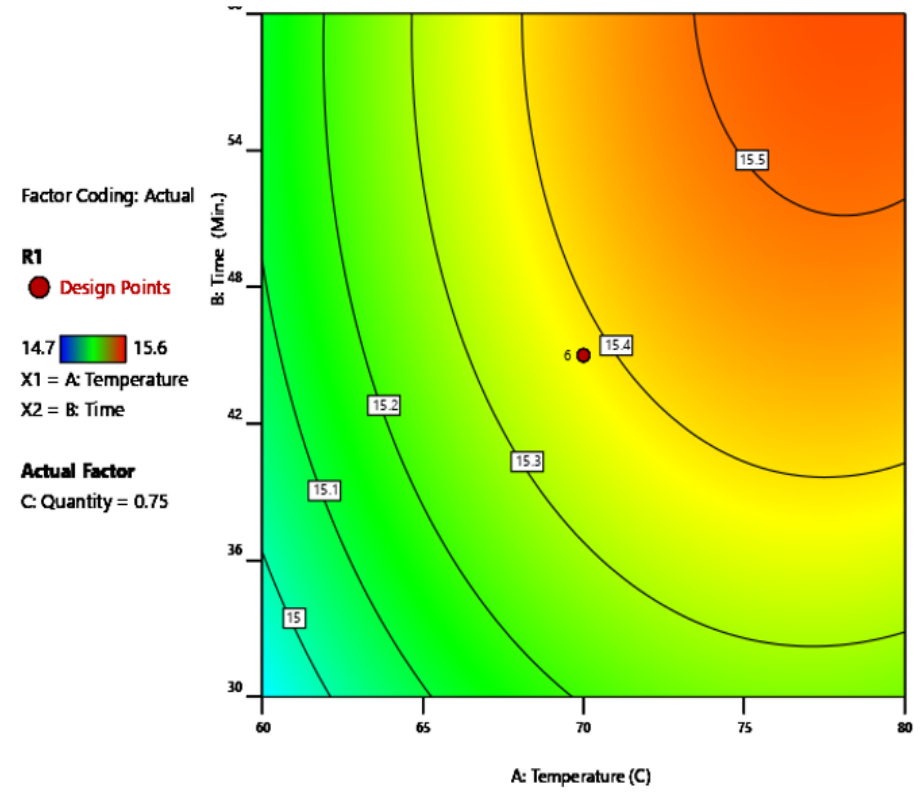

Fig. 7. The contour plot representing the interactions of the terms A: Temperature and B: Time for the SPME technique using Design-Expert software (after exerting model reduction approach).

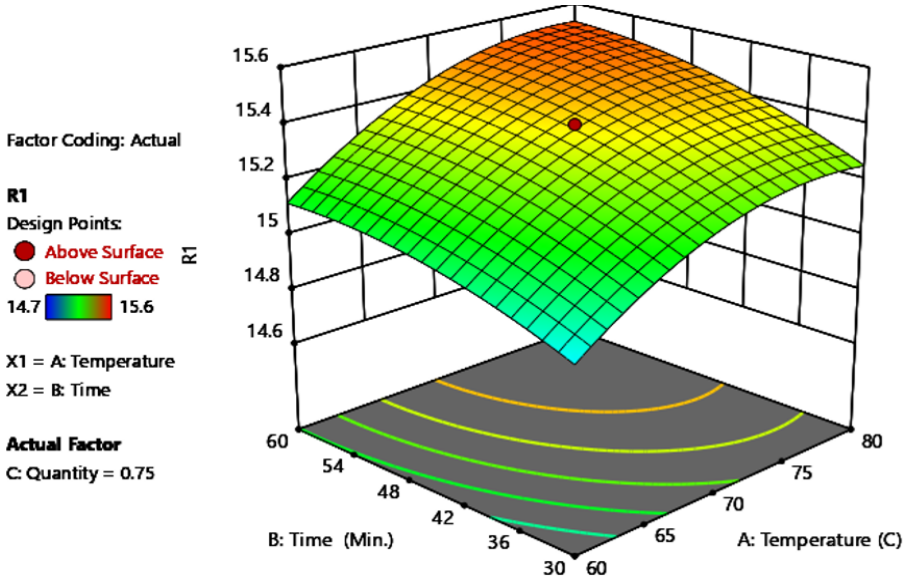

Fig. 8. The 3D surface plot representing the interactions of the terms A: Temperature and B: Time for the SPME technique using Design-Expert software (after exerting model reduction approach).

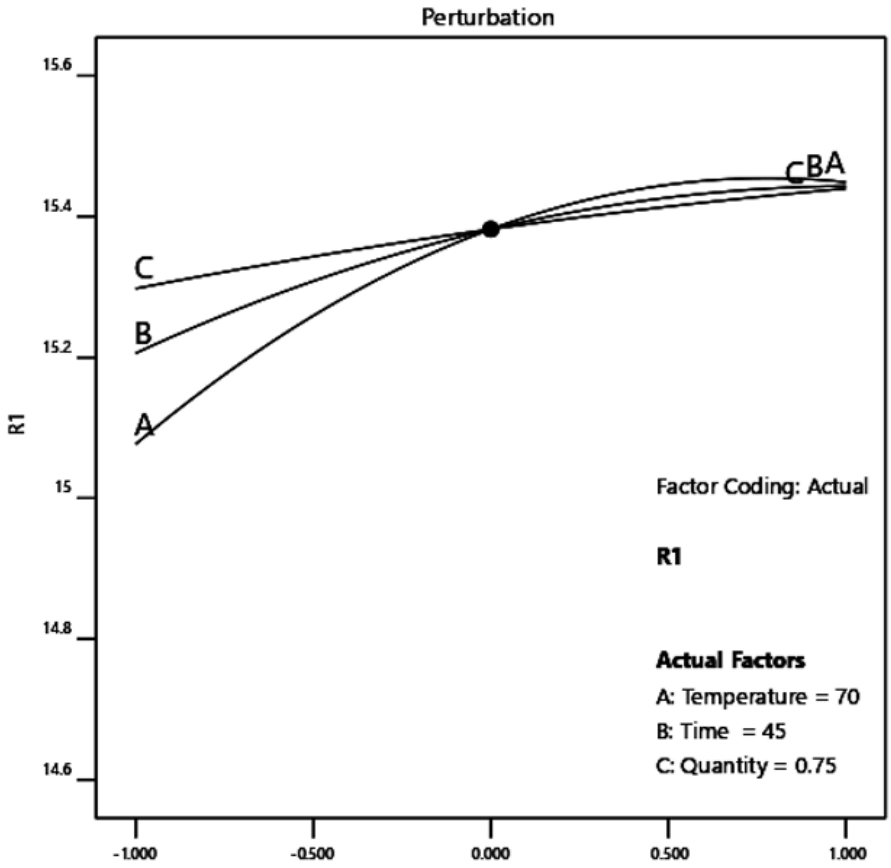

Fig. 9. The disturbtion plot drawn by Design-Expert software of the proposed SPME approach.

4. Concluding remarks

In the recent decades, HS-SPME-GC/MS has gained much attention for the quantitative and qualitative analysis of a large number of volatiles, more specifically, the plant volatile fractions. Our study on the volatile fractions obtained from the flowers, leaves, stems and roots of *Allium tripedale* Trautv. revealed that sulfur-containing compounds, *e.g.*, diallyl tetrasulfide, methyl allicin, diallyl thiosulfinate (allicin), and diallyl disulfide (DAS) connstituted most of the chemical profiles. The general impact of the experimental parameters, involving temperature (°C), conditioning time (min.) and the quantity of the plant material (g) has been evaluated and optimized using Design-Expert software. In the second part of this investigation, the methanol extracts from a mixture of the stems and the leaves of *A. tripedale* Trautv have been prepared by the use of maceration, Soxhlet and ultrasonic approaches. Different biological activities of these extracts involving antioxidant, *e.g.*, DPPH assay, total phenolic content (TPC), total flavonoid content (TFC), and ferrous ion chelating (FIC) assay along with antibacterial activities, using disk diffusion method and minimum inhibitory concentration (MIC) approach have also been assessed.

List of abbreviations

***A. sativum* L.:** *Allium sativum* L.; ***Allium tripedale* Trautv.:** *A. tripedale* Trautv.; **ANOVA:** Analysis of Variance; **AscA:** Ascorbic Acid; **BHT:** Butylated Hydroxytoluene; **CCD:** Central Composite Design; **CitA:** Citric Acid; **DAS:** Diallyl Disulfide; **DOE:** Design of Experiment; **DPPH:** 2,2-Diphenyl-1-Picrylhydrazyl Radical; **EDTA:** Ethylenediaminetetraacetic Acid; ***Enterococcus faecalis*:** *E. faecalis*; ***Escherichia coli*:** *E. coli*; **FCR:** Folin-Ciocalteu Reagent; **Ferrozine:** 3-(2-Pyridyl)-5,6-Diphenyl-1,2,4-Triazine-*P*,*P'*-Disulfonic Acid Monosodium Salt; **FIC:** Ferrous Ion Chelating; **FID:** Flame Ionization Detector; **GA:** Gallic acid; **GC/MS:** Gas Chromatography-Mass Spectrometry; **GCA:** Gas Chromatographic Analyses; **GC-O:** Gas Chromatography-Olfactometry; **HS-SPME:** Headspace Solid Phase Microextraction; **HS-SPME-GC/MS:** Headspace-Solid Phase Microextraction-Gas Chromatography-Mass Spectrometry; **IC_{50}:** Half-Maximal Inhibitory Concentration; **IZD:** Inhibition Zone Diameter; ***Klebsiella* pneumoniae:** *K. pneumonioae*; **LDL:** Low-Density Lipoprotein; **MH:** Monoterpene Hydrocarbon; **MHB:** Mueller-Hinton Broth; **MIC:** Minimum Inhibitory Concentration; **NH:** Non-Terpene Hydrocarbon;**OAVs:** Odor Activity Values; **OM:** Oxygenated Monoterpene; **OS:** Oxygenated Sesquiterpene; **PCA:** Principal Component Analysis; **PDMS-CAR:** Polydimethylsiloxane-Carboxen; **PLS-DA:** Partial Least Squares Discriminant Analysis; **PLSR:** Partial Least Squares Regression; ***Proteus vulgaris*:** *P. vulgaris*; ***Pseudomonas aeruginosa*:** *P. aeruginosa*; **Q-Q Plot:** Normal Quantile Plot; **R&O-CCD:** Rotatable And Orthogonal Central Composite Design; **RP-HPLC:** Reverse Phase-High Performance Liquid Chromatography; **RSA:** Radical Scavenging Activity; **RSM:** Response Surface Methodology; **Ru:** Rutin; ***S. aureus*:** *Staphylococcus aureus*; **SD:** Standard Deviations; **SH:** Sesquiterpene Hydrocarbon; ***Staphylococcus coagulase*:** *S. coagulase*; **TFC:** Total Flavonoid Content; **TPC:** Total Phenolic Content; **λ:** Lambda.

Author contribution statement

Conceptualization and literature search were performed by Mousa Gholami, Behnam Mahdavi and Majid Mohammadhosseini. The first draft of the manuscript was prepared by Behnam Mahdavi. Majid Mohammadhosseini critically analyzed and gave suggestions to finalize the manuscript. All authors read and approved the final manuscript.

Conflict of interest

The authors declare that there is no conflict of interest.

Acknowledgements

Financial and technical supports of Department of Chemistry, Faculty of Science, Hakim Sabzevari University, Sabzevar, Iran as well as Islamic Azad University of Shahrood are gratefully acknowledged.

References

Adhikari, D., Rangra, N., 2023. Antimicrobial activities of *Acacia* genus: A review. Asian Pac. J. Trop. Biomed. 13(2), 45-59.

Aggarwal, G., Sharma, M., Singh, R., Sharma, U., 2024. Ethnopharmacologically important highly subsidized Indian medicinal plants: Systematic review on their traditional uses, phytochemistry, pharmacology, quality control, conservation status and future prospective. J. Ethnopharmacol. 320, doi: 10.1016/j.jep.2023.117385.

Al-Kubeisi, A.K., 2022. Evaluation of antibacterial activity of aqueous and alcohol extracts of *Zingiber officinale* and *Allium sativum* on bacterial isolates from urinary tract infection patients. Int. J. Drug Deliv. Technol. 12(4), 1751-1756.

AlAgha, I., Elshawa, A., Alhayek, G., Ghabayen, M., Alkhattib, R., 2023. PalAST: A cross-platform mobile application for automated disk diffusion antimicrobial susceptibility testing. Int. J. Interact. Mob. Technol. 17(22), 85-99.

Amalia, N., Okta, F.N., Zahra, A.A., Nuari, D.A., 2024. Update review: Extraction, purification, and pharmacological activities of Gotu Kola terpenoids. Lett. Appl. NanoBioSci. 13(1), doi: 10.33263/LIANBS131.006.

Anusha, K., Balakrishnan, S., Sindhu, S., Hariram, S.B., 2014. Screening the metal chelating efficacy of *Trichodesma Indicum*. Res. J. Pharm., Biol. Chem. Sci. 5(2), 1259-1262.

Arment, S., 1999. Automated soxhlet extraction. LC GC: Liquid Chromatography, Gas Chromatography 17(6 SUPPL.), S38-S42.

Atkinson, A.C., Riani, M., Corbellini, A., 2021. The Box–Cox transformation: Review and extensions. Stat. Sci. 36(2), 239-255.

Ayala, A., Munoz, M.F., Arguelles, S., 2014. Lipid

peroxidation: Production, metabolism, and signaling mechanisms of malondialdehyde and 4-hydroxy-2-nonenal. Oxid. Med. Cell. Longev. 2014, 360438.
Bhaskaracharya, R.K., Kentish, S., Ashokkumar, M., 2009. Selected applications of ultrasonics in food processing. Food. Eng. Rev. 1(1), 31-49.
Biancolillo, A., Aloia, R., Rossi, L., D'Archivio, A.A., 2022. Organosulfur volatile profiles in Italian red garlic (*Allium sativum* L.) varieties investigated by HS-SPME/GC-MS and chemometrics. Food Control 131, doi: 10.1016/j.foodcont.2021.108477.
Bienvenu, A.L., Leboucher, G., Picot, S., 2019. Comparison of fks gene mutations and minimum inhibitory concentrations for the detection of *Candida glabrata* resistance to micafungin: A systematic review and meta-analysis. Mycoses 62(9), 835-846.
Biscay Lirio, R., Valdés Sosa, P.A., Pascual Marqui, R.D., Jiménez-Sobrino, J.C., Alvarez Amador, A., Galán Garcia, L., 1989. Multivariate Box-Cox transformations with applications to neurometric data. Comput. Biol. Med. 19(4), 263-267.
Boshra, Y.R., Fahim, J.R., Hamed, A.N.E., Desoukey, S.Y., 2022. Phytochemical and biological attributes of *Narcissus pseudonarcissus* L. (Amaryllidaceae): A review. S. Afr. J. Bot. 146, 437-458.
Chagas, A.G.D.R., Spinelli, E., Souza, T.M., Pinto Junior, J.A., Pereira Netto, A.D., 2019. Simultaneous determination of alpha-, beta- and gamma-hydroxybutyric acids in micro-pulverized human hair by GC-MS: Method development, validation and application. Talanta 194, 576-584.
Chaudry, A.E., Klausner, J.D., 2021. A narrative review of clinical treatment outcomes of *Neisseria gonorrhoeae* infection with ciprofloxacin by minimum inhibitory concentration and anatomic site. Sex. Transm. Dis. 48(6), 385-392.
D'Auria, M., Racioppi, R., 2017. HS-SPME-GC-MS analysis of onion (*Allium cepa* L.) and shallot (*Allium ascalonicum* L.). Food Res. 1(5), 161-165.
Dadashpour, M., Rasooli, I., Sefidkon, F., Taghizadeh, M., Darvish Alipour Astaneh, S.H., 2011. Comparison of ferrous ion chelating, free radical scavenging and anti tyrosinase properties of *Thymus daenensis* essential oil with commercial thyme oil and thymol. J. Zanjan Univ. Med. Sci. Health Serv. 19(77), 41-52.
Dalton, B.R., 2023. What is the best vancomycin therapeutic drug monitoring parameter to assess efficacy? A critical review of experimental data and assessment of the need for individual patient minimum inhibitory concentration value. Microorg. 11(3), doi: 10.3390/microorganisms11030567.
Dalton, B.R., Rajakumar, I., Langevin, A., Ondro, C., Sabuda, D., Griener, T.P., Dersch-Mills, D., Rennert-May, E., 2020. Vancomycin area under the curve to minimum inhibitory concentration ratio predicting clinical outcome: A systematic review and meta-analysis with pooled sensitivity and specificity. Clin. Microbiol. Infect. 26(4), 436-446.
Desgagné-Penix, I., 2021. Biosynthesis of alkaloids in Amaryllidaceae plants: A review. Phytochem. Rev. 20(2), 409-431.
Dias, P.G.I., Sajiwanie, J.W.A., Rathnayaka, R.M.U.S.K., Awolu, O.O., 2021. Optimization of composite fruit peel powder as a texture modifier for fat free set yoghurt: A mixture design approach. J. Agri. Sci. Sri. Lanka 16(2), 226-236.
Dreger, M., Adamczak, A., Foksowicz-Flaczyk, J., 2023. Antibacterial and antimycotic activity of *Epilobium angustifolium* L. extracts: A review. Pharmaceuticals 16(10), doi: 10.3390/ph16101419.
Ebadi, Z., Ghaisari, H., Tajeddin, B., Shekarforoush, S.S., 2022. Evaluation of the properties and antibacterial activity of microchitosan film impregnated with Shirazi thyme (*Zataria multiflora*) and garlic (*Allium sativum*) essential oils. Iran. J. Vet. Res. 23(1), 53-60.
El Jabboury, Z., Bentaib, R., Stevanovic, Z.D., Ousaaid, D., Benjelloun, M., El Ghadraoui, L., 2023. *Ammi visnaga* (L.) Lam.: An overview of phytochemistry and biological functionalities. Trends Phytochem. Res. 7(3), 141-155.
Feyisa, K., Yismaw, M.B., Yehualaw, A., Tafere, C., Demsie, D.G., Bahiru, B., Kefale, B., 2024. Medicinal plants traditionally used to treat human ailments in Ethiopia: A systematic review. Phytomed. Plus 4(1), doi: 10.1016/j.phyplu.2023.100516.
Gangaram, T., Mohan Naidu, G., Balasiddamuni, P., 2014. Some alternative tests for heteroscedasticity using studentized and predicted residuals. Int. J. Agric. Stat. Sci. 10(1), 111-114.
Ghaffari, H., Sadeghi Dinani, M., 2018. Isolation of phenyl propanoid glycosides from *Allium tripedale* Trautv. J. Rep. Pharm. Sci. 7(2), 116-122.
Ghobadi, S., Dastan, D., Soleimani, M., Nili-Ahmadabadi, A., 2019. Hepatoprotective potential and antioxidant activity of *Allium tripedale* in acetaminophen-induced oxidative damage. Res. Pharm. Sci. 14(6), 488-495.
Gupta, M., Kumar, A., 2019. Comparison of minimum inhibitory concentration (MIC) value of statin drugs: A systematic review. Anti-Infect. Agents 17(1), 4-19.
Jaillais, B., Cadoux, F., Auger, J., 1999. SPME-HPLC analysis of *Allium* lacrymatory factor and thiosulfinates. Talanta 50(2), 423-431.
Kalil, A.C., Van Schooneveld, T.C., Fey, P.D., Rupp, M.E., 2014. Association between vancomycin minimum inhibitory concentration and mortality among patients with *Staphylococcus aureus* bloodstream infections: A systematic review and meta-analysis. JAMA 312(15), 1552-1564.
Keusgen, M., 2011. Volatile Compounds of the Genus *Allium* L.(Onions), Volatile Sulfur Compounds in Food. ACS Publications, pp. 183-214.
Kim, M.G., 2017. A cautionary note on the use of Cook's distance. Commun. Stat. Appl. Methods 24(3), 317-324.
Kim, N.Y., Park, M.H., Jang, E.Y., Lee, J., 2011. Volatile distribution in garlic (*Allium sativum* L.) by solid phase microextraction (SPME) with different processing conditions. Food Sci. Biotechnol. 20(3), 775-782.
Kiokias, S., Proestos, C., Oreopoulou, V., 2018. Effect of natural food antioxidants against LDL and DNA oxidative changes. Antioxidants 7(10), 133.
Laksmiani, N.P.L., Vidya Paramita, N.L.P., Wirasuta, I.M.A.G., 2016. *In vitro* and *in silico* antioxidant activity of purified fractions from purple sweet potato ethanolic

extract. Int. J. Pharmcy Pharm. Sci. 8(8), 177-181.
Lamaison, J., Carnet, A., 1990. Teneurs en principaux flavonoids des fleurs de *Crataegeus monogyna* Jacq et de *Crataegeus laevigata* (Poiret D. C) en fonction de la vegetation. Pharm. Acta Helv. 65, 315-320.
Leszczyńska, D., Hallmann, A., Treder, N., Bączek, T., Roszkowska, A., 2024. Recent advances in the use of SPME for drug analysis in clinical, toxicological, and forensic medicine studies. Talanta 270, doi: 10.1016/j.talanta.2023.125613.
Li, F., Yang, W., Yang, M., Wang, Y., Zhang, J., 2024. Differences between two plants fruits: *Amomum tsaoko* and *Amomum maximum*, using the SPME-GC–MS and FT-NIR to classification. Arab. J. Chem. 17(4), doi: 10.1016/j.arabjc.2024.105665.
Luque de Castro, M.D., García-Ayuso, L.E., 1998. Soxhlet extraction of solid materials: An outdated technique with a promising innovative future. Anal. Chim. Acta 369(1-2), 1-10.
Luque de Castro, M.D., Priego-Capote, F., 2010. Soxhlet extraction: Past and present panacea. J. Chromatogr. A 1217(16), 2383-2389.
Mahdavi, B., Mohammadhosseini, M., 2022. Antioxidant, antimicrobial and anti-prostate cancer activity of the extracts from different parts of *Etlingera velutina* (Ridl.) R. M. Sm (Zingiberaceae). Trends Phytochem. Res. 6(4), 353-362.
Martín, N., 2015. Diagnostics in a simple correspondence analysis model: An approach based on Cook's distance for log-linear models. J. Multivariate Anal. 136, 175-189.
Martín, N., Pardo, L., 2009. On the asymptotic distribution of Cook's distance in logistic regression models. J. Appl. Stat. 36(10), 1119-1146.
Mohammadhosseini, M., Jeszka-Skowron, M., 2023. A systematic review on the ethnobotany, essential oils, bioactive compounds, and biological activities of *Tanacetum* species. Trends Phytochem. Res. 7(1), 1-29.
Morgan, E., 1991. Chemometrics: Experimental Design. John Wiley, London.
Mozuraityte, R., Kristinova, V., Rustad, T., 2016. Encyclopedia of Food and Health. Academic Press Oxford, UK.
Murti, Y., Singh, S., Pathak, K., 2024. Classical Techniques for Extracting Essential Oils from Plants, Essential Oils: Extraction Methods and Applications. Wiley, pp. 795-858.
Najafi, F., Zangeneh, M.M., Tahvilian, R., Zangeneh, A., Amiri, H., Amiri, N., Moradi, R., 2016. *In vitro* antibacterial efficacy of essential oil of *Allium sativum* against *Staphylococcus aureus*. Int. J. Pharmacogn. Phytochem. Res. 8(12), 2039-2043.
Nnamchi, C.I., Okefum, V.E., Amaechi, C.D., Ugwu, K., Nsofor, C.A., 2021. Antibacterial and synergistic effects of extracts of allium *cepa*, *Alium sativum*, zingiber officinale and garcinia kola on selected bacterial strains. Trop. J. Nat. Prod. Res. 5(4), 763-771.
Obradović, D., Komsta, Ł., Agbaba, D., 2020. Novel computational approaches to retention modeling in dual hydrophilic interactions/reversed phase chromatography. J. Chromatogr. A 1619.
Ortega-Ramirez, L.A., Silva-Espinoza, B.A., Vargas-Arispuro, I., Gonzalez-Aguilar, G.A., Cruz-Valenzuela, M.R., Nazzaro, F., Ayala-Zavala, J.F., 2016. Combination of cymbopogon citrates and *Allium cepa* essential oils increased antibacterial activity in leafy vegetables. J. Sci. Food Agric. 97(7), 2166-2173.
Otunola, G.A., Afolayan, A.J., Ajayi, E.O., Odeyemi, S.W., 2017. Characterization, antibacterial and antioxidant properties of silver nanoparticles synthesized from aqueous extracts of *Allium sativum*, Zingiber officinale, and Capsicum frutescens. Pharmacogn. Mag. 13(50), S201-S208.
Ourouadi, S., Hasib, A., El Mahi, F., 2022. Evaluation of biochemical, antioxidant and antibacterial activities of garlic extracts (*Allium sativum*. L) grown in five Moroccan eco-regions. Moroc. J. Chem. 10(4), 761-771.
Pandey, A.K., Sara, U.S., 2023. Quality by design approach for optimization of 5-fluorouracil microbeads using box–behnken design and desirability function for colon targeting. J. Pharm. Innov. 18(4), 2054-2065.
Pinho, L.G.B., Nobre, J.S., Singer, J.M., 2015. Cook's distance for generalized linear mixed models. Comput. Stat. Data Anal. 82, 126-136.
Rahn, K., 1998. Alliaceae, Flowering Plants· Monocotyledons: Lilianae (Except Orchidaceae). Springer, pp. 70-78.
Rajasekar, A., Moorthi, M., Deivasigamani, P., Sekar, S., Amar, G., 2023. A Review on Screening, Isolation, and Characterization of Phytochemicals in Plant Materials: Methods and Techniques, Pharmacological Benefits of Natural Agents. IGI Global, pp. 1-12.
Rivera, A., Viñado, B., Benito, N., Docobo-Pérez, F., Fernández-Cuenca, F., Fernández-Domínguez, J., Guinea, J., López-Navas, A., Moreno, M.Á., Larrosa, M.N., Oliver, A., Navarro, F., 2023. Recommendations of the Spanish antibiogram committee (COESANT) for *in vitro* susceptibility testing of antimicrobial agents by disk diffusion. Enferm. Infecc. Microbiol. Clin. 41(9), 571-576.
Rofouei, M.K., Kojoori, S.M.H., Moazeni-Pourasil, R.S., 2021. Optimization of chlorogenic acid extraction from Elm tree, Ulmus minor Mill., fruits, using response surface methodology. Sep. Purif. Technol. 256, 117773.
Samura, M., Kitahiro, Y., Tashiro, S., Moriyama, H., Hamamura, Y., Takahata, I., Kawabe, R., Enoki, Y., Taguchi, K., Takesue, Y., Matsumoto, K., 2022. Efficacy and safety of daptomycin versus vancomycin for bacteremia caused by methicillin-resistant *Staphylococcus aureus* with vancomycin minimum inhibitory concentration > 1 microg/mL: A systematic review and meta-analysis. Pharmaceutics 14(4), doi: 10.3390/pharmaceutics14040714.
Sen, T., Samanta, S.K., 2014. Medicinal plants, human health and biodiversity: A broad review. Adv. Biochem. Eng. Biotechnol. 147, 59-110.
Shi, C., Ye, J., Xu, R., Jin, W., Xu, S., Teng, F., Lin, N., 2021. Effect of the vancomycin minimum inhibitory concentration on clinical outcomes in patients with methicillin-susceptible *Staphylococcus aureus* bacteraemia: A systematic review and meta-analysis. BMJ Open 11(1), e040675.
Singh, D., Mittal, N., Siddiqui, M.H., 2023. A review on pharmacological potentials of phenolic diterpenes

carnosic acid and carnosol obtained from *Rosmarinus officinalis* L. and modern extraction methods implicated in their recovery. Trends Phytochem. Res. 7(3), 156-169.
Singleton, V.L., Orthofer, R., Lamuela-Raventós, R.M., 1999. Analysis of total phenols and other oxidation substrates and antioxidants by means of Folin-Ciocalteu reagent. Methods Enzymol. 299, 152-178.
Stan, M., Popa, A., Toloman, D., Silipas, T.D., Vodnar, D.C., 2016. Antibacterial and antioxidant activities of ZnO nanoparticles synthesized using extracts of *Allium sativum*, *Rosmarinus officinalis* and *Ocimum basilicum*. Acta Metal. Sin. 29(3), 228-236.
Taiyari, H., Faiz, N.M., Abu, J., Zakaria, Z., 2021. Antimicrobial minimum inhibitory concentration of *Mycoplasma gallisepticum*: A systematic review. J. Appl. Poult. Res. 30(2), doi: 10.1016/j.japr.2021.100160.
Takahashi, M., 2022. A new robust ratio estimator by modified Cook's distance for missing data imputation. Jpn. J. Stat. Data. Sci. 5(2), 783-830.
Tang, J., Zhu, X., Jambrak, A.R., Sun, D.-W., Tiwari, B.K., 2023. Mechanistic and synergistic aspects of ultrasonics and hydrodynamic cavitation for food processing. Crit. Rev. Food Sci. Nutr., 1-22, doi: 10.1080/10408398.2023.2201834.
Torres, E., Delgado, M., Valiente, A., Pascual, Á., Rodríguez-Baño, J., 2015. Impact of borderline minimum inhibitory concentration on the outcome of invasive infections caused by Enterobacteriaceae treated with β-lactams: A systematic review and meta-analysis. Eur. J. Clin. Microbiol. Infect. Dis. 34(9), 1751-1758.
Van de Vel, E., Sampers, I., Raes, K., 2019. A review on influencing factors on the minimum inhibitory concentration of essential oils. Crit. Rev. Food Sci. Nutr. 59(3), 357-378.
Van Hal, S.J., Lodise, T.P., Paterson, D.L., 2012. The clinical significance of vancomycin minimum inhibitory concentration in *Staphylococcus aureus* infections: A systematic review and meta-analysis. Clin. Infect. Dis. 54(6), 755-771.
Van Otterlo, W.A.L., Green, I.R., 2018. A review on recent syntheses of amaryllidaceae alkaloids and isocarbostyrils (time period mid-2016 to 2017). Nat. Prod. Comm. 13(3), 255-277.
Wieczorek, M.N., Zhou, W., Jeleń, H.H., Pawliszyn, J., 2024. Automated sequential SPME addressing the displacement effect in food samples. Food Chem. 439, doi: 10.1016/j.foodchem.2023.138093.
Xiang, G., Guo, S., Qin, J., Gao, H., Zhang, Y., Wang, S., 2024. Comprehensive insight into the pharmacology, pharmacokinetics, toxicity, detoxification and extraction of hypaconitine from *Aconitum* plants. J. Ethnopharmacol. 321, 117505.
Xie, B., Wu, Q., Wei, S., Li, H., Wei, J., Hanif, M., Li, J., Liu, Z., Xiao, X., Yu, J., 2022. Optimization of headspace solid-phase micro-extraction conditions (HS-SPME) and Identification of major volatile aroma-active compounds in Chinese chive (*Allium tuberosum* Rottler). Molecules 27(8), doi: 10.3390/molecules27082425.
Yerbanga, I.W., Nakanabo Diallo, S., Rouamba, T., Resendiz-Sharpe, A., Lagrou, K., Denis, O., Rodriguez-Villalobos, H., Montesinos, I., Bamba, S., 2023. Performances of disk diffusion method for determining triazole susceptibility of *Aspergillus* species: Systematic review. J. Med. Mycol. 33(4), doi: 10.1016/j.mycmed.2023.101413.
Yeşilyurt, V., Halfon, B., Öztürk, M., Topçu, G., 2008. Antioxidant potential and phenolic constituents of *Salvia cedronella*. Food Chem. 108(1), 31-39.
Yin, J., Wu, T., Zhu, B., Cui, P., Zhang, Y., Chen, X., Ding, H., Han, L., Bie, S., Li, F., Song, X., Yu, H., Li, Z., 2024. Comprehensive multicomponent characterization and quality assessment of Xiaoyao Wan by UPLC-Q-Orbitrap-MS, HS-SPME-GC-MS and HS-GC-IMS. J. Pharm. Biomed. Anal. 239, doi: 10.1016/j.jpba.2023.115910.
Zabihi, A., Akhondzadeh Basti, A., Amoabediny, G., Khanjari, A., Tavakkoly Bazzaz, J., Mohammadkhan, F., Hajjar Bargh, A., Vanaki, E., 2017. Physicochemical characteristics of nanoliposome garlic (*Allium sativum* L.) Essential Oil and its antibacterial effect on Escherichia coli O157:H7. J. Food Qual. Hazards Control 4(1), 24-28.
Zeaiter, M., Roger, J.M., Bellon-Maurel, V., Rutledge, D.N., 2004. Robustness of models developed by multivariate calibration. Part I: The assessment of robustness. TrAC Trends Anal. Chem. 23(2), 157-170.
Zhang, C., Wang, Y., Ding, D., Su, J., Zhao, Z., 2022a. Volatile profiles of *Allium tenuissimum* L. flower fried by four different oils, using SPME–GC–MS, and sensory evaluation coupled with partial least squares regression. J. Food Compos. Anal. 109, doi: 10.1016/j.jfca.2022.104461.
Zhang, S., Hou, Q., Fu, Z., Jiang, H., 2022b. Multi-response optimization of thermal cycling process for Al6092/SiC/ZrW_2O_8 composites using RSM-MOGA. Arab. J. Sci. Eng. 47(6), 7669-7682.